

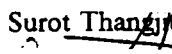
In-Plane Vibrations of a Transversely Isotropic Arch

by

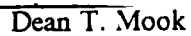
Sandra Lynn Scrivener

Thesis submitted to the Faculty of the
Virginia Polytechnic Institute and State University
in partial fulfillment of the requirements for the degree of
Master of Science
in
Engineering Mechanics

APPROVED:


Surot Thangjitham, Chairman


Robert A. Heller


Dean T. Mook


O. Hayden Griffin

July, 1989

Blacksburg, Virginia

In-Plane Vibrations of a Transversely Isotropic Arch

by

Sandra Lynn Scrivener

Surot Thangjitham, Chairman

Engineering Mechanics

(ABSTRACT)

A model for the dynamic response of a laminated composite arch is developed from classical shell theory. The problem is reduced from a shell to an arch by making an assumption that the variation of the field of variables in the direction of the width of the arch is small compared to those in other directions. Standard separation of variables is used to change from a system of partial differential equations to that of ordinary differential equations. Several methods of solution are explored, namely the Laplace transformation, the method of particular solutions, and the eigensolution. The eigensolution is chosen as the most efficient in terms of computer time and is the easiest to modify. The free vibration of the arch is explored and the natural frequencies of the system are determined. The response of the arch to general forcing functions is also considered, by the use of the Fourier transformation technique. Damping through material viscoelasticity and use of the model in evaluation of experimental data are also discussed.

Table of Contents

List of Illustrations	iv
List of Tables	v
Chapter 1	1
INTRODUCTION	1
DIMENSIONS AND ASSUMPTIONS	4
Chapter 2	10
EQUATIONS OF MOTION	10
COMPARISONS	22
Chapter 3	26
SOLUTION TECHNIQUES	26
Laplace Transformations	26
The Method of Particular Solutions	29
Eigensolution	34
Table of Contents	iii

Comparison of Results	35
Chapter 4	39
RESULTS	39
Free Vibrations	39
FORCED RESPONSE	40
Frequency Response Function	52
Fourier Transformations	60
Chapter 5	70
SPECIAL TOPICS	70
Viscoelasticity	70
Determination of Modulus	71
Conclusions	81
Bibliography	83
Additional Reading	84
Appendix A	88
Derivation of [Q]	88
Appendix B	90
Program for Determination of Modulus	90
Vita	100

List of Illustrations

Figure 1. Three-dimensional arch	5
Figure 2. Coordinates in polar and shell reference frames	6
Figure 3. Comparison of normalized frequencies	37
Figure 4. v , w , and w' versus theta, composite	41
Figure 5. v , w , and w' versus theta, isotropic	42
Figure 6. v , w , and w' versus theta, composite	43
Figure 7. v , w , and w' versus theta, isotropic	44
Figure 8. v , w , and w' versus theta, composite	45
Figure 9. v , w , and w' versus theta, isotropic	46
Figure 10. Total displacement	47
Figure 11. Total displacement	48
Figure 12. Total displacement	49
Figure 13. Total displacement	50
Figure 14. Arch	51
Figure 15. Resonance peak	59
Figure 16. $F_{sub 1}(t)$	64
Figure 17. $F_{sub 2}(t)$	65
Figure 18. $F_{sub 3}(t)$	66
Figure 19. Frequency response function	67
Figure 20. Radial response	69
Figure 21. Damped Resonance Peak	72

Figure 22. Phase shift	73
Figure 23. Damped response for F1	74
Figure 24. Damped response for F2	75
Figure 25. Damped response for F3	76
Figure 26. ω_1 vs E_{θ}	78
Figure 27. Data from a DMA test	79
Figure 28. E_{θ} vs temperature	80

List of Tables

Table 1. Eigensolution	36
Table 2. Normalized Frequencies	38
Table 3. Sample Input	98
Table 4. Sample Output	99

Chapter 1

INTRODUCTION

The history of composite materials is long and varied. Recent developments in the field have gained widespread acceptance by engineers and others as high performance structural components. Composite materials are defined as being composed of two or more materials that are joined together in such a way that the components retain their integrity. This results in a new material possessing properties that cannot be achieved by using the components separately. The idea of composite materials is not new. Composites have been in use throughout history, from early times when bricks were made from straw and mud, to the modern use of concrete, which is made up of a load-bearing component, rocks and sand, and an adhesive, cement. More sophisticated is the idea of reinforced concrete, which has steel bars embedded in concrete. Employing the same principle, on a smaller scale, are fiber reinforced composite materials, which consist of load bearing parts, usually fibers, embedded in an adhesive, generally an epoxy resin. A common arrangement is to have long continuous fibers oriented in a single direction, which results in a material that is very strong in the direction of the fibers, but rather weak in a transverse direction. To counteract this drawback, layers of fibers can be placed in varying directions, to yield a material which can have a

wide range of material properties, depending on the orientation of the fibers within it. This ability to manipulate the material properties of the final product is one of the characteristics which makes composites such an attractive structural material to today's designer. Also, in its precured state, the material is rather flexible and easy to manipulate, so that parts that previously had to be machined separately and then assembled can be made as one piece with a minimum of wasted material and post processing assembly.

Modern fiber reinforced-composites, made with fibers such as graphite or Kevlar, are lighter and stronger than conventional materials such as aluminum or steel. While raw material costs are higher, there are cost-effective applications in high-performance fields, such as military aircraft and space structures, where weight reduction is at a premium. The benefits of these materials were apparent very quickly, and once sufficient technology was established to guarantee a continuous market and supply, production and applications of composites accelerated. Composites have been the subject of intense research in the last decade or so, because they are so different from conventional materials. Despite all the attention focused on the mechanics of composite materials, the technology and applications based on them continues to accelerate beyond the current scope of understanding, and so it remains a dynamic and expanding field of study.

As mentioned before, one of the more appealing characteristics of composite materials is their capacity for being formed into parts that would generally require extensive machining and/or assembly. In addition to the complex micromechanics involved, the structural analysis of these parts must also include the behavior of unusually shaped pieces. Many of these analyses are possible only through numerical techniques such as finite element modeling, or other "mathematical disassembly" of the structure. Unfortunately, analytic models are available only for the simplest of composite structural components. One of the most obvious omissions from this list of available models is one for a composite arch.

Curved panels are an important structural element of many composite components, such as fuselages or motor casings. While the whole assembly is more properly modeled as a cylinder, some test specimens must be modeled as rings or arches. These components frequently are subject to their greatest stresses at dynamic, rather than static, loads, and so it is the material properties under these

conditions that are most critical. One piece of test equipment that is designed to determine the dynamic properties of a specimen is the Dynamic Mechanical Analyzer (DMA). This is a system designed by DuPont, and can give such information as the storage and shear moduli, along with a measure of the damping inherent in a material under given conditions. To test a particular material, it is necessary to obtain a small specimen from the structure. However, when the structure in question is round, such as is the case with a rocket motor casing, the sample from the circumference is necessarily curved, and in this case was a complete semi-circle. This led to problems with the DMA, because it is part of a complete data-analysis program set up for flat rectangular specimens.

The material used in the test consisted of a semi-circle made up of fibers running in the circumferential direction, held together by an epoxy or other bonding agent. The properties of this material, particularly the modulus of elasticity and the amount of damping present under a dynamic load, were investigated. The input parameters to the DMA were modified to correct for the extra length of a curved specimen, and the system was excited at resonance.

To account for arch mechanics, above and beyond the extra specimen length, and to incorporate the anisotropy of the material, a model was required for a composite arch, subject to the excitation like that induced by the DMA. Upon investigation, very few, if any, models for the vibrations of a composite arch were found in the literature, and none was applicable to the immediate problem.

The model that is developed in Chapters 2 and 3 is based on shell theory. The equations of motion are compared to shell equations derived by two different methods. In Chapter 4, the resulting solution to the free-vibration problem is compared with existing solutions for an isotropic arch and with data from vibration testing of other composite arches. Upon obtaining reasonable agreement with these sources, the forced-vibration case is solved, up to and including general forcing functions, to complete the problem solution. Chapter 5 contains a discussion of the results of the model as they apply to interpreting the DMA data, along with a brief explanation of the damping mechanism employed in the model and its effects on the arch response. Finally, a list of sources for additional reading on the vibration of arches is included in addition to the references in the bibliography which were used directly in developing the model.

DIMENSIONS AND ASSUMPTIONS

The test specimen was modeled as a semicircular arch, as shown in Fig. 1, with radius R , clamped at both ends, and subjected to a steady harmonic excitation at one end of the form $A e^{i\Omega t}$, where Ω is the excitation frequency, and A is the amplitude of excitation. The coordinates are z , θ and x . The dimensions of the arch are h in the z direction, i.e., the thickness of the arch, a in the x direction, and 0 to π radians in the θ direction. The displacements are u in the x direction, v in the tangential direction, and w in the radial direction. The equations of motion were derived using the classical theory of elasticity and minimization of the system energy by using Hamilton's principle. The following assumptions were made in the derivation.

1. $h \ll R$.
2. u and v are linear functions of z .
3. h and R are constant.
4. The strains associated with the z direction; ϵ_z , $\epsilon_{z\theta}$, and ϵ_{zz} , are negligible with respect to the other strains.
5. Rotatory inertia and shear deformation are neglected.
6. There are no body forces.

Polar displacements in the coordinate system as shown in Fig. 2 are given by [1]:

$$u = u^o - z \frac{\partial w^o}{\partial x}, \quad v = v^o \left(1 + \frac{z}{R}\right) - \frac{z}{R} \frac{\partial w^o}{\partial \theta}, \quad w = w^o \quad (1)$$

where u^o , v^o , and w^o are the midplane displacements in the x , θ , and z directions, respectively.

Using the classical linear theory of elasticity, the strain-displacement relationships are given by [2]:

$$\epsilon_x = \frac{\partial u}{\partial x}, \quad \epsilon_\theta = \frac{w}{r} + \frac{1}{r} \frac{\partial v}{\partial \theta}, \quad \epsilon_{x\theta} = \frac{\partial v}{\partial x} + \frac{1}{r} \frac{\partial u}{\partial \theta} \quad (2)$$

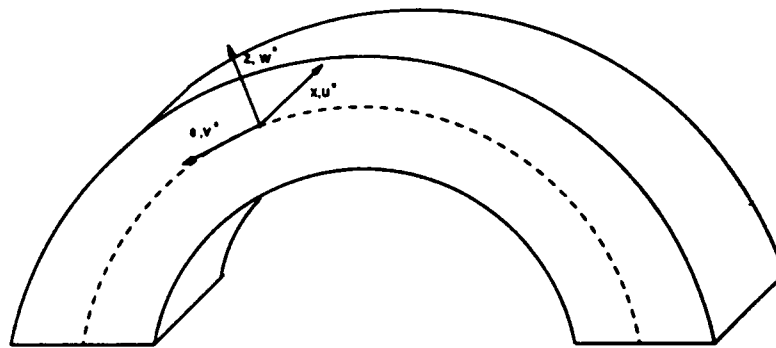
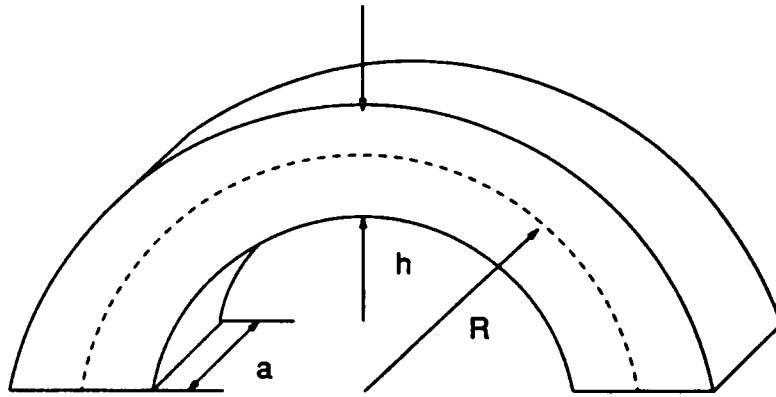


Figure 1. Three-dimensional arch

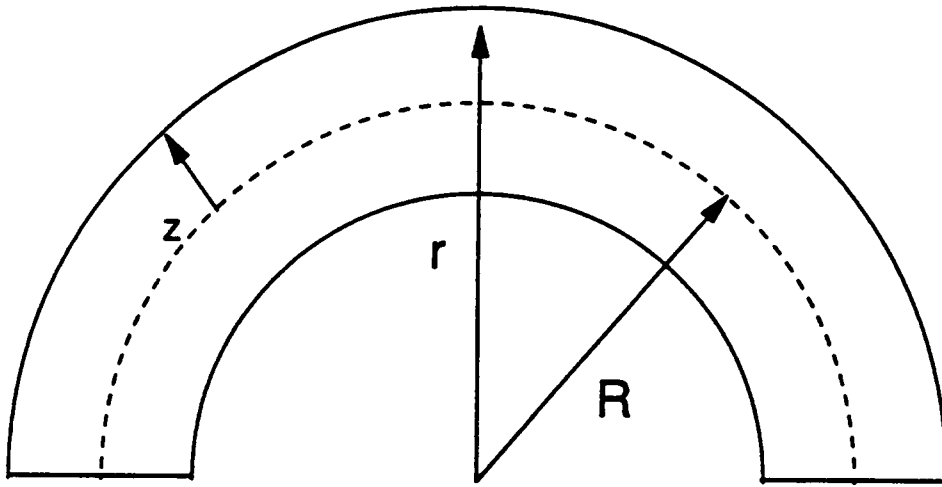


Figure 2. Coordinates in polar and shell reference frames

where ε_x and ε_θ are the normal strains in the indicated directions, $\varepsilon_{x\theta}$ is the shear strain between the x and θ planes, and r is the running variable, defined by $r = R + z$

Substituting the displacements in terms of the midplane quantities, Eq. (1), into the strain displacement equations, Eq. (2) yields:

$$\varepsilon_x = \frac{\partial u^o}{\partial x} - z \frac{\partial^2 w^o}{\partial x^2}, \quad \varepsilon_\theta = \frac{w^o}{r} + \frac{R+z}{rR} \frac{\partial v^o}{\partial \theta} - \frac{z}{rR} \frac{\partial^2 w^o}{\partial \theta^2},$$

$$\varepsilon_{x\theta} = \frac{1}{r} \frac{\partial u^o}{\partial \theta} + \left(1 + \frac{z}{R}\right) \frac{\partial v^o}{\partial x} - \left(\frac{z}{R} + \frac{z}{r}\right) \frac{\partial^2 w^o}{\partial x \partial \theta} \quad (3)$$

When the the Saunder's approximation, [3], is applied, $R + z = r \approx R$ these relationships simplify to:

$$\varepsilon_x = \frac{\partial u^o}{\partial x} - z \frac{\partial^2 w^o}{\partial x^2}, \quad \varepsilon_\theta = \frac{1}{R} \frac{\partial v^o}{\partial \theta} + \frac{w^o}{R} - \frac{z}{R^2} \frac{\partial^2 w^o}{\partial \theta^2},$$

$$\varepsilon_{x\theta} = \frac{1}{R} \frac{\partial u^o}{\partial \theta} + \frac{\partial v^o}{\partial x} - \frac{2z}{R} \frac{\partial^2 w^o}{\partial x \partial \theta} \quad (4)$$

These expressions in terms of the midplane strains, ε^o , and midplane curvatures, κ are:

$$\varepsilon_x = \varepsilon_x^o + z \kappa_x, \quad \varepsilon_\theta = \varepsilon_\theta^o + z \kappa_\theta, \quad \varepsilon_{x\theta} = \varepsilon_{x\theta}^o + z \kappa_{x\theta}, \quad (5)$$

where

$$\varepsilon_x^o = \frac{\partial u^o}{\partial x}, \quad \varepsilon_\theta^o = \frac{1}{R} \left(\frac{\partial v^o}{\partial \theta} + w^o \right), \quad \varepsilon_{x\theta}^o = \frac{1}{R} \frac{\partial u^o}{\partial \theta} + \frac{\partial v^o}{\partial x}$$

$$\kappa_x = -\frac{\partial^2 w^o}{\partial x^2}, \quad \kappa_\theta = -\frac{1}{R^2} \frac{\partial^2 w^o}{\partial \theta^2}, \quad \kappa_{x\theta} = -\frac{2}{R} \frac{\partial^2 w^o}{\partial x \partial \theta} \quad (6)$$

By employing Hooke's law for plane stress, the stress-strain relations can be written as [4]:

$$\begin{bmatrix} \sigma_x \\ \sigma_\theta \\ \sigma_{x\theta} \end{bmatrix} = \begin{bmatrix} Q_{11} & Q_{12} & Q_{16} \\ Q_{12} & Q_{22} & Q_{26} \\ Q_{16} & Q_{26} & Q_{66} \end{bmatrix} \begin{bmatrix} \varepsilon_x \\ \varepsilon_\theta \\ \varepsilon_{x\theta} \end{bmatrix} \quad (7)$$

where σ_x , σ_θ , and $\sigma_{x\theta}$ are the stresses in the x , θ , and $x\theta$ directions, and the Q_{ij} are the elements of the reduced stiffness matrix. This matrix is derived in detail in Appendix A.

As in classical lamination theory, the resultant in-plane forces and resultant moments can be defined as, [4]:

$$N_x, N_\theta, N_{x\theta} = \int_{-\frac{h}{2}}^{+\frac{h}{2}} (\sigma_x, \sigma_\theta, \sigma_{x\theta}) dz \quad \text{and} \quad M_x, M_\theta, M_{x\theta} = \int_{-\frac{h}{2}}^{+\frac{h}{2}} (\sigma_x, \sigma_\theta, \sigma_{x\theta}) z dz \quad (8)$$

where N_x, N_θ , and $N_{x\theta}$ are the resultant forces per unit length in the directions indicated by the subscripts, and M_x, M_θ , and $M_{x\theta}$ are the resultant moments in the directions indicated by the subscripts.

The derived midplane strains and curvatures from Eq. (5) are substituted into Eq. (7), that expression substituted into Eq. (8), and the integral is taken with respect to z . Then the resulting relationships can be written:

$$\begin{bmatrix} N \\ \dots \\ M \end{bmatrix} = \begin{bmatrix} A & | & B \\ \dots & \dots & \dots \\ B & | & D \end{bmatrix} \begin{bmatrix} \varepsilon^o \\ \dots \\ \kappa \end{bmatrix} \quad (8)$$

where

$$N = [N_x \ N_\theta \ N_{x\theta}]^T \quad \text{and} \quad M = [M_x \ M_\theta \ M_{x\theta}]^T$$

$$A_{ij}, B_{ij}, D_{ij} = \int_{-\frac{h}{2}}^{+\frac{h}{2}} Q_{ij} (1, z, z^2) dz \quad (9)$$

for which A_{ij} are elements of the extensional stiffness matrix, $[A]$, B_{ij} are elements of the bend-twist coupling matrix, $[B]$, and D_{ij} are elements of the bending stiffness matrix, $[D]$. For special cases with certain symmetries, such as an orthotropic or isotropic material, many of the elements of these matrices are identically equal to zero.

Chapter 2

EQUATIONS OF MOTION

There are several ways of determining the governing equations of motion for shells. It is possible to use the three-dimensional theory of elasticity [3], or the theory used in curved beams and bars [5], or the principle of minimization of system energy [2]. All of these methods should agree, to a certain extent, depending on the consistency of the assumptions employed in each formulation. The method chosen in this study is the minimization of total system energy because it is relatively rigorous and yields the necessary boundary conditions. The resulting equations are compared to those derived using modified beam and bar theory, and the results from those different derivations are also compared and discussed.

The relevant quantities in this formulation are the potential energy due to strain and the kinetic energy of motion. The strain energy, $U^{(k)}$, for the k th lamina, written in terms of the reduced stiffness matrix and the strains, is:

$$U^{(k)} = \frac{1}{2} \int \int \int \{ Q_{11}^{(k)} \varepsilon_x^2 + 2 Q_{12}^{(k)} \varepsilon_\theta \varepsilon_x + 2 Q_{16}^{(k)} \varepsilon_x \varepsilon_{x\theta} + 2 Q_{26}^{(k)} \varepsilon_\theta \varepsilon_{x\theta} +$$

$$Q_{22}^{(k)} \varepsilon_{\theta}^2 + Q_{66}^{(k)} \varepsilon_{x\theta}^2 \} R dz d\theta dx \quad (10)$$

Substituting in the strain-displacement relations from Eq. (4) into Eq. (10) yields:

$$\begin{aligned} U^{(k)} = & \frac{1}{2} \int \int \int \left[Q_{11}^{(k)} \left\{ \left(\frac{\partial u^o}{\partial x} \right)^2 + 2z \left(\frac{\partial^2 w^o}{\partial x^2} \right) \left(\frac{\partial u^o}{\partial x} \right) + z^2 \left(-\frac{\partial^2 w^o}{\partial x^2} \right)^2 \right\} \right. \\ & + 2Q_{12}^{(k)} \left\{ \frac{1}{R} \left(\frac{\partial u^o}{\partial x} \right) \left(\frac{\partial v^o}{\partial \theta} + w^o \right) \right. \\ & \left. \left. + z \left[\frac{1}{R^2} \left(\frac{\partial u^o}{\partial x} \right) \left(-\frac{\partial^2 w^o}{\partial \theta^2} \right) + \frac{1}{R} \left(\frac{\partial v^o}{\partial \theta} + w^o \right) \left(-\frac{\partial^2 w^o}{\partial x^2} \right) \right] \right\} \right. \\ & + 2Q_{12}^{(k)} \left\{ \frac{z^2}{R^2} \left(-\frac{\partial^2 w^o}{\partial x^2} \right) \left(-\frac{\partial^2 w^o}{\partial \theta^2} \right) \right\} + 2Q_{16}^{(k)} \left\{ \left(\frac{\partial u^o}{\partial x} \right) \left(\frac{1}{R} \frac{\partial u^o}{\partial \theta} + \frac{\partial v^o}{\partial x} \right) \right\} \\ & + 2Q_{16}^{(k)} \left\{ z \left[\frac{1}{R} \left(\frac{\partial u^o}{\partial x} \right) \left(-\frac{\partial^2 w^o}{\partial x \partial \theta} \right) + \left(\frac{1}{R} \frac{\partial u^o}{\partial \theta} + \frac{\partial v^o}{\partial \theta} \right) \left(-\frac{\partial^2 w^o}{\partial x^2} \right) \right] \right\} \\ & + 2Q_{16}^{(k)} \left\{ \frac{z^2}{R^2} \left(-\frac{\partial^2 w^o}{\partial x^2} \right) \left(-\frac{\partial^2 w^o}{\partial x \partial \theta} \right) \right\} \\ & + 2Q_{26}^{(k)} \left\{ \frac{1}{R} \left(\frac{\partial v^o}{\partial \theta} + w^o \right) \left(\frac{1}{R} \frac{\partial u^o}{\partial \theta} + \frac{\partial v^o}{\partial x} \right) \right\} \\ & + 2Q_{26}^{(k)} \left\{ z \left[\frac{1}{R^2} \left(\frac{1}{R} \frac{\partial u^o}{\partial \theta} + \frac{\partial v^o}{\partial x} \right) \left(-\frac{\partial^2 w^o}{\partial \theta^2} \right) \right] \right\} \\ & \left. + 2Q_{26}^{(k)} \left\{ z \left[+ \frac{1}{R^2} \left(-\frac{\partial^2 w^o}{\partial x \partial \theta} \right) \left(\frac{\partial v^o}{\partial \theta} + w^o \right) \right] \right\} \right] \end{aligned}$$

$$\begin{aligned}
& + 2 Q_{26}^{(k)} \left\{ \frac{z^2}{R^3} \left(-\frac{\partial^2 w^o}{\partial \theta^2} \right) \left(-\frac{\partial^2 w^o}{\partial x \partial \theta} \right) \right\} \\
& + Q_{22}^{(k)} \left\{ \frac{1}{R^2} \left(\frac{\partial v^o}{\partial \theta} + w^o \right)^2 + \frac{2z}{R} \left(\frac{\partial v^o}{\partial \theta} + w^o \right) \left(-\frac{\partial^2 w^o}{\partial \theta^2} \right) \right\} \\
& + Q_{22}^{(k)} \left\{ + \frac{z^2}{R^4} \left(-\frac{\partial^2 w^o}{\partial \theta^2} \right)^2 \right\} \\
& + Q_{66}^{(k)} \left\{ \left(\frac{1}{R} \frac{\partial u^o}{\partial \theta} + \frac{\partial v^o}{\partial x} \right)^2 + \frac{2z}{R} \left(\frac{1}{R} \frac{\partial u^o}{\partial \theta} + \frac{\partial v^o}{\partial x} \right) \left(-\frac{\partial^2 w^o}{\partial x \partial \theta} \right) \right\} \\
& + Q_{66}^{(k)} \left\{ \frac{z^2}{R^2} \left(-\frac{\partial^2 w^o}{\partial x \partial \theta} \right)^2 \right\} \Big] R dz d\theta dx \tag{11}
\end{aligned}$$

Integrating with respect to z gives the total system energy U for the shell and yields an expression in terms of $[A]$, $[B]$, and $[D]$, the matrices described in Eq. (9).

$$\begin{aligned}
U = \frac{1}{2} \int \int \left\{ & A_{11} \left(\frac{\partial u^o}{\partial x} \right)^2 + 2 B_{11} \left(-\frac{\partial^2 w^o}{\partial x^2} \right) \left(\frac{\partial u^o}{\partial x} \right) + D_{11} \left(-\frac{\partial^2 w^o}{\partial x^2} \right)^2 \right. \\
& + 2 A_{12} \frac{1}{R} \left(\frac{\partial u^o}{\partial x} \right) \left(\frac{\partial v^o}{\partial \theta} + w^o \right) + D_{12} \frac{1}{R^2} \left(-\frac{\partial^2 w^o}{\partial x^2} \right) \left(-\frac{\partial^2 w^o}{\partial \theta^2} \right) \\
& + B_{12} \left[\frac{1}{R^2} \left(\frac{\partial u^o}{\partial x} \right) \left(-\frac{\partial^2 w^o}{\partial \theta^2} \right) + \frac{1}{R} \left(\frac{\partial v^o}{\partial \theta} + w^o \right) \left(-\frac{\partial^2 w^o}{\partial x^2} \right) \right] \\
& + 2 A_{16} \left(\frac{\partial u^o}{\partial x} \right) \left(\frac{1}{R} \frac{\partial u^o}{\partial \theta} + \frac{\partial v^o}{\partial x} \right) + D_{16} \frac{1}{R^2} \left(-\frac{\partial^2 w^o}{\partial x^2} \right) \left(-\frac{\partial^2 w^o}{\partial x \partial \theta} \right) \\
& \left. + B_{16} \left[\frac{1}{R} \left(\frac{\partial u^o}{\partial x} \right) \left(-\frac{\partial^2 w^o}{\partial x \partial \theta} \right) + \left(\frac{1}{R} \frac{\partial u^o}{\partial \theta} + \frac{\partial v^o}{\partial x} \right) \left(-\frac{\partial^2 w^o}{\partial x^2} \right) \right] \right\}
\end{aligned}$$

$$\begin{aligned}
& + 2A_{26} \frac{1}{R} \left(\frac{\partial v^o}{\partial \theta} + w^o \right) \left(\frac{1}{R} \frac{\partial u^o}{\partial \theta} + \frac{\partial v^o}{\partial \theta} \right) + D_{26} \frac{1}{R^3} \left(-\frac{\partial^2 w^o}{\partial \theta^2} \right) \left(-\frac{\partial^2 w^o}{\partial x \partial \theta} \right) \\
& + B_{26} \left[\frac{1}{R^2} \left(\frac{1}{R} \frac{\partial u^o}{\partial \theta} + \frac{\partial v^o}{\partial x} \right) \left(-\frac{\partial^2 w^o}{\partial \theta^2} \right) + \frac{1}{R^2} \left(-\frac{\partial^2 w^o}{\partial x \partial \theta} \right) \left(\frac{\partial v^o}{\partial \theta} + w^o \right) \right] \\
& + A_{22} \frac{1}{R^2} \left(\frac{\partial v^o}{\partial \theta} + w^o \right)^2 + B_{22} \frac{2}{R} \left(\frac{\partial v^o}{\partial \theta} + w^o \right) \left(-\frac{\partial^2 w^o}{\partial \theta^2} \right) \\
& + D_{22} \frac{1}{R^4} \left(-\frac{\partial^2 w^o}{\partial \theta^2} \right)^2 + A_{66} \left(\frac{1}{R} \frac{\partial u^o}{\partial \theta} + \frac{\partial v^o}{\partial x} \right)^2 \\
& + B_{66} \frac{2}{R} \left(\frac{1}{R} \frac{\partial u^o}{\partial \theta} + \frac{\partial v^o}{\partial x} \right) \left(-\frac{\partial^2 w^o}{\partial x \partial \theta} \right) + D_{66} \frac{1}{R^2} \left(-\frac{\partial^2 w^o}{\partial x \partial \theta} \right)^2 \} R \, d\theta \, dx \quad (12)
\end{aligned}$$

The kinetic energy of the system, T , is:

$$T = \frac{1}{2} \iint \rho \left[\left(\frac{\partial u^o}{\partial t} \right)^2 + \left(\frac{\partial v^o}{\partial t} \right)^2 + \left(\frac{\partial w^o}{\partial t} \right)^2 \right] dx \, d\theta \quad (13)$$

where t is time, and ρ , the mass per unit area, is defined in terms of the mass per unit volume of the k th layer, $\rho^{(k)}$ as:

$$\rho = \int_{-\frac{h}{2}}^{+\frac{h}{2}} \rho^{(k)} \, dz \quad (14)$$

Once these expressions are inserted into Hamilton's principle, the energy is minimized by taking the first variation of the expression. Then the arbitrariness of the virtual displacements is invoked to yield the desired equations of motion and the boundary conditions.

Hamilton's principle as applied to this problem is:

$$\delta I = \delta \int_{t_1}^{t_2} L dt = 0 \quad (15)$$

where L is the Lagrangian, defined as: $L = T - U$ subject to

$$\delta u^o, \delta v^o, \text{ and } \delta w^o = 0 \text{ at } t = t_1 \text{ and } t = t_2 \quad (16)$$

for which δu^o , δv^o , and δw^o are virtual displacements.

Taking the first variation of the potential energy and regrouping the resulting terms leaves:

$$\begin{aligned} \delta U = & \int_0^a \int_0^\pi \left[\left\{ A_{11} \left(\frac{\partial u^o}{\partial x} \right) + \frac{A_{12}}{R} \left(\frac{\partial v^o}{\partial \theta} + w^o \right) \right. \right. \\ & \left. \left. + A_{16} \left(\frac{1}{R} \frac{\partial u^o}{\partial \theta} + \frac{\partial v^o}{\partial x} \right) \right\} \frac{\partial}{\partial x} \delta u^o \right] \\ & - \left\{ B_{11} \left(\frac{\partial^2 w^o}{\partial x^2} \right) + \frac{B_{12}}{R^2} \left(\frac{\partial^2 w^o}{\partial x^2} \right) + 2 B_{16} \left(\frac{\partial^2 w^o}{\partial x \partial \theta} \right) \right\} \frac{\partial}{\partial x} \delta u^o \\ & + \left\{ A_{12} \left(\frac{\partial u^o}{\partial x} \right) + \frac{A_{22}}{R} \left(\frac{\partial v^o}{\partial \theta} + w^o \right) \right. \\ & \left. + A_{26} \left(\frac{1}{R} \frac{\partial u^o}{\partial \theta} + \frac{\partial v^o}{\partial x} \right) \right\} \left\{ \frac{1}{R} \left(\frac{\partial}{\partial \theta} \delta v^o + \delta w^o \right) \right\} \\ & - \left\{ B_{12} \left(\frac{\partial^2 w^o}{\partial x^2} \right) + \frac{B_{22}}{R^2} \left(\frac{\partial^2 w^o}{\partial \theta^2} \right) + 2 \frac{B_{26}}{R} \left(\frac{\partial^2 w^o}{\partial x \partial \theta} \right) \right\} \left\{ \frac{1}{R} \left(\frac{\partial}{\partial \theta} \delta v^o + \delta w^o \right) \right\} \\ & \left\{ A_{16} \left(\frac{\partial u^o}{\partial x} \right) + \frac{A_{26}}{R} \left(\frac{\partial v^o}{\partial \theta} + w^o \right) \right\} \end{aligned}$$

$$\begin{aligned}
& + A_{66} \left(\frac{1}{R} \frac{\partial u^o}{\partial \theta} + \frac{\partial v^o}{\partial x} \right) \left\{ \left(\frac{1}{R} \frac{\partial}{\partial \theta} \delta u^o + \frac{\partial}{\partial x} \delta v^o \right) \right. \\
& - \left\{ B_{16} \left(\frac{\partial^2 w^o}{\partial x^2} \right) + \frac{B_{26}}{R^2} \left(\frac{\partial^2 w^o}{\partial \theta^2} \right) + 2 \frac{B_{66}}{R} \left(\frac{\partial^2 w^o}{\partial x \partial \theta} \right) \right\} \left(\frac{1}{R} \frac{\partial}{\partial \theta} \delta u^o + \frac{\partial}{\partial x} \delta v^o \right) \\
& - \left\{ B_{11} \left(\frac{\partial u^o}{\partial x} \right) + \frac{B_{12}}{R} \left(\frac{\partial v^o}{\partial \theta} + w^o \right) + B_{16} \left(\frac{1}{R} \frac{\partial u^o}{\partial \theta} + \frac{\partial v^o}{\partial x} \right) \right\} \left(\frac{\partial^2}{\partial x^2} \delta w^o \right) \\
& \left\{ D_{11} \left(\frac{\partial^2 w^o}{\partial x^2} \right) + \frac{D_{12}}{R^2} \left(\frac{\partial^2 w^o}{\partial \theta^2} \right) + 2 \frac{D_{16}}{R} \left(\frac{\partial^2 w^o}{\partial x \partial \theta} \right) \right\} \left(\frac{\partial^2}{\partial x^2} \delta w^o \right) \\
& - \left\{ B_{12} \left(\frac{\partial u^o}{\partial x} \right) + \frac{B_{22}}{R} \left(\frac{\partial v^o}{\partial \theta} + w^o \right) \right. \\
& \left. + B_{26} \left(\frac{1}{R} \frac{\partial u^o}{\partial \theta} + \frac{\partial v^o}{\partial x} \right) \right\} \left(\frac{1}{R^2} \frac{\partial^2}{\partial \theta^2} \delta w^o \right) \\
& \left\{ D_{12} \left(\frac{\partial^2 w^o}{\partial x^2} \right) + \frac{D_{22}}{R^2} \left(\frac{\partial^2 w^o}{\partial \theta^2} \right) + 2 \frac{D_{26}}{R} \left(\frac{\partial^2 w^o}{\partial x \partial \theta} \right) \right\} \left(\frac{1}{R^2} \frac{\partial^2}{\partial \theta^2} \delta w^o \right) \\
& - \left\{ 2 B_{16} \left(\frac{\partial u^o}{\partial x} \right) + 2 \frac{B_{26}}{R} \left(\frac{\partial v^o}{\partial \theta} + w^o \right) \right. \\
& \left. + 2 B_{66} \left(\frac{1}{R} \frac{\partial u^o}{\partial \theta} + \frac{\partial v^o}{\partial x} \right) \right\} \left(\frac{1}{R} \frac{\partial^2}{\partial x \partial \theta} \delta w^o \right) \\
& \left\{ 2 D_{16} \left(\frac{\partial^2 w^o}{\partial x^2} \right) + 2 \frac{D_{26}}{R^2} \left(\frac{\partial^2 w^o}{\partial \theta^2} \right) \right. \\
& \left. + 2 \frac{D_{66}}{R} \left(\frac{\partial^2 w^o}{\partial x \partial \theta} \right) \right\} \left(\frac{1}{R} \frac{\partial^2}{\partial x \partial \theta} \delta w^o \right) \Big] dx R d\theta \tag{17}
\end{aligned}$$

Writing this in terms of the in-plane forces and moments results in a simpler expression. In this form the equations appear as:

$$\delta U = \int_0^a \int_0^\pi \left[N_x \left(\frac{\partial}{\partial x} \delta u^o \right) + \frac{N_\theta}{R} \left(\frac{\partial}{\partial \theta} \delta v^o + \delta w^o \right) + N_{x\theta} \left(\frac{1}{R} \frac{\partial}{\partial \theta} \delta u^o + \frac{\partial}{\partial x} \delta v^o \right) - M_x \left(\frac{\partial^2}{\partial x^2} \delta w^o \right) - \frac{M_\theta}{R^2} \left(\frac{\partial^2}{\partial \theta^2} \delta w^o \right) - \frac{2 M_{x\theta}}{R} \left(\frac{\partial^2}{\partial x \partial \theta} \delta w^o \right) \right] dx R d\theta \quad (18)$$

In order to isolate the variational displacements, it is necessary to integrate by parts, term by term. The individual steps in this process are not shown here; the end result is:

$$\begin{aligned} \delta U = & \int_0^a \int_0^\pi \left[\left(- \frac{\partial}{\partial x} N_x - \frac{1}{R} \frac{\partial}{\partial \theta} N_{x\theta} \right) \delta u^o \right. \\ & + \left(- \frac{1}{R} \frac{\partial}{\partial \theta} N_\theta - \frac{\partial}{\partial x} N_{x\theta} \right) \delta v^o \\ & \left. \left(- \frac{\partial^2}{\partial x^2} M_x - \frac{1}{R^2} \frac{\partial^2}{\partial \theta^2} M_\theta - \frac{1}{R} \frac{\partial^2}{\partial x \partial \theta} 2 M_{x\theta} + \frac{N_\theta}{R} \right) \delta w^o \right] dx R d\theta \\ & + \int_0^\pi \left[N_x \delta u^o \Big|_0^a + \frac{1}{R} N_{x\theta} \delta v^o \Big|_0^a - M_x \frac{\partial}{\partial x} \delta w^o \Big|_0^a \right. \\ & \left. + \frac{\partial}{\partial x} (M_x) \delta w^o \Big|_0^a - \frac{2}{R} M_{x\theta} \frac{\partial}{\partial \theta} \delta w^o \Big|_0^a \right] R d\theta \\ & - \int_0^a \left[N_\theta \delta v^o \Big|_0^\pi + N_{x\theta} \delta u^o \Big|_0^\pi - \frac{1}{R} M_\theta \frac{\partial}{\partial \theta} \delta w^o \Big|_0^\pi \right] R d\theta \end{aligned}$$

$$+ \frac{1}{R} \frac{\partial}{\partial \theta} (M_\theta) \delta w^\circ \Big|_0^\pi + \frac{2}{R} \frac{\partial}{\partial x} (M_{x\theta}) \delta w^\circ \Big|_0^\pi \Big] dx \quad (19)$$

The variation of kinetic energy can be developed in a similar fashion. The final result of that variation is:

$$\delta T = \int_0^a \int_0^\pi -\rho \left[\left(\frac{\partial^2 u^\circ}{\partial t^2} \right) \delta u^\circ + \left(\frac{\partial^2 v^\circ}{\partial t^2} \right) \delta v^\circ + \left(\frac{\partial^2 w^\circ}{\partial t^2} \right) \delta w^\circ \right] dx R d\theta \quad (20)$$

These variational forms are now inserted into Hamilton's equation to yield:

$$\begin{aligned} & \int_{t_1}^{t_2} \int_0^a \int_0^\pi \left[\left\{ \frac{\partial}{\partial x} N_x + \frac{1}{R} \frac{\partial}{\partial \theta} N_{x\theta} - \left(\frac{\partial^2 u^\circ}{\partial t^2} \right) \right\} \delta u^\circ \right. \\ & + \left\{ \frac{1}{R} \frac{\partial}{\partial \theta} N_\theta + \frac{\partial}{\partial x} N_{x\theta} - \left(\frac{\partial^2 v^\circ}{\partial t^2} \right) \right\} \delta v^\circ \\ & + \left[\frac{\partial^2}{\partial x^2} M_x + \frac{1}{R^2} \frac{\partial^2}{\partial \theta^2} M_\theta + \frac{1}{R} \frac{\partial^2}{\partial x \partial \theta} 2 M_{x\theta} \right. \\ & \left. \left. - \frac{N_\theta}{R} - \left(\frac{\partial^2 w^\circ}{\partial t^2} \right) \right] \delta w^\circ \right] dx R d\theta dt \end{aligned}$$

$$\begin{aligned} & - \int_{t_1}^{t_2} \int_0^\pi \left[N_x \delta u^\circ \Big|_0^a + \frac{1}{R} N_{x\theta} \delta v^\circ \Big|_0^a - M_x \frac{\partial}{\partial x} \delta w^\circ \Big|_0^a \right. \\ & \left. + \frac{\partial}{\partial x} (M_x) \delta w^\circ \Big|_0^a - \frac{2}{R} M_{x\theta} \frac{\partial}{\partial \theta} \delta w^\circ \Big|_0^a \right] R d\theta dt \end{aligned}$$

$$\int_{t_1}^{t_2} \int_0^a \left[N_\theta \delta v^o \Big|_0^\pi + N_{x\theta} \delta u^o \Big|_0^\pi - \frac{1}{R} M_\theta \frac{\partial}{\partial \theta} \delta w^o \Big|_0^\pi \right. \\ \left. + \frac{1}{R} \frac{\partial}{\partial \theta} (M_\theta) \delta w^o \Big|_0^\pi + \frac{2}{R} \frac{\partial}{\partial x} (M_{x\theta}) \delta w^o \Big|_0^\pi \right] dx dt = 0 \quad (21)$$

The only way for this expression to hold for all cases is for all the coefficients of the virtual displacements to be identically equal to zero, which yields the three equations of motion, and for the boundary terms to be also equal to zero, independently. That is to say, every term, in addition to the sum of terms, is constrained to be zero. These terms yield the necessary boundary conditions. The resulting equations of motion are:

$$\frac{\partial}{\partial x} N_x + \frac{1}{R} \frac{\partial}{\partial \theta} N_{x\theta} = \frac{\partial^2 u^o}{\partial t^2} \quad (22)$$

$$\frac{1}{R} \frac{\partial}{\partial \theta} N_\theta + \frac{\partial}{\partial x} N_{x\theta} = \frac{\partial^2 v^o}{\partial t^2} \quad (23)$$

$$\frac{\partial^2}{\partial x^2} M_x + \frac{1}{R^2} \frac{\partial^2}{\partial \theta^2} M_\theta + \frac{1}{R} \frac{\partial^2}{\partial x \partial \theta} 2 M_{x\theta} - \frac{N_\theta}{R} = \frac{\partial^2 w^o}{\partial t^2} \quad (24)$$

The required boundary conditions are:

$$N_x \delta u^o \Big|_0^a = 0 \quad N_{x\theta} \delta v^o \Big|_0^a = 0$$

$$M_x \frac{\partial}{\partial x} \delta w^o \Big|_0^a = 0 \quad \frac{\partial}{\partial x} (M_x) \delta w^o \Big|_0^a = 0$$

$$M_{x\theta} \frac{\partial}{\partial \theta} \delta w^o \Big|_0^a = 0 \quad N_\theta \delta v^o \Big|_0^\pi = 0$$

$$N_{x\theta} \delta u^o \Big|_0^\pi = 0 \quad M_\theta \frac{\partial}{\partial \theta} \delta w^o \Big|_0^\pi = 0$$

$$\frac{\partial}{\partial \theta} (M_\theta) \delta w^o \Big|_0^\pi = 0 \quad \frac{\partial}{\partial x} (M_{x\theta}) \delta w^o \Big|_0^\pi = 0 \quad (25)$$

The equations of motion, in terms of the components of the $[A]$, $[B]$, and $[D]$ matrices, are:

$$\begin{aligned} & A_{11} \frac{\partial^2 u^o}{\partial x^2} + \frac{A_{12}}{R} \left(\frac{\partial^2 v^o}{\partial x \partial \theta} + \frac{\partial w^o}{\partial x} \right) + A_{16} \left(\frac{2}{R} \frac{\partial^2 u^o}{\partial x \partial \theta} + \frac{\partial^2 v^o}{\partial x^2} \right) \\ & + \frac{A_{26}}{R^2} \left(\frac{\partial^2 v^o}{\partial \theta^2} + \frac{\partial w^o}{\partial \theta} \right) + \frac{A_{66}}{R} \left(\frac{1}{R} \frac{\partial^2 u^o}{\partial \theta^2} + \frac{\partial^2 v^o}{\partial \theta \partial x} \right) - B_{11} \left(\frac{\partial^3 w^o}{\partial x^3} \right) \\ & - \frac{B_{12}}{R^2} \left(\frac{\partial^3 w^o}{\partial x \partial \theta^2} \right) \\ & - \frac{3 B_{16}}{R} \left(\frac{\partial^3 w^o}{\partial \theta \partial x^2} \right) - \frac{B_{26}}{R^3} \left(\frac{\partial^3 w^o}{\partial \theta^3} \right) - \frac{2 B_{66}}{R^2} \left(\frac{\partial^3 w^o}{\partial x \partial \theta^2} \right) = \rho \frac{\partial^2 u^o}{\partial t^2} \end{aligned} \quad (26)$$

$$\begin{aligned} & \frac{A_{12}}{R} \left(\frac{\partial^2 u^o}{\partial x \partial \theta} \right) + \frac{A_{22}}{R^2} \left(\frac{\partial^2 v^o}{\partial \theta^2} + \frac{\partial w^o}{\partial \theta} \right) + \frac{A_{26}}{R} \left(\frac{1}{R} \frac{\partial^2 u^o}{\partial \theta^2} + 2 \frac{\partial^2 v^o}{\partial \theta \partial x} + \frac{\partial w^o}{\partial x} \right) \\ & + A_{16} \left(\frac{\partial^2 u^o}{\partial x^2} \right) + A_{66} \left(\frac{1}{R} \frac{\partial^2 u^o}{\partial x \partial \theta} + \frac{\partial^2 v^o}{\partial x^2} \right) - \frac{B_{12}}{R} \left(\frac{\partial^3 w^o}{\partial \theta \partial x^2} \right) \\ & - \frac{B_{22}}{R^3} \left(\frac{\partial^3 w^o}{\partial \theta^3} \right) - \frac{3 B_{26}}{R^2} \left(\frac{\partial^3 w^o}{\partial x \partial \theta^2} \right) \\ & - B_{16} \left(\frac{\partial^3 w^o}{\partial x^3} \right) - \frac{2 B_{26}}{R} \left(\frac{\partial^3 w^o}{\partial x^2 \partial \theta} \right) = \rho \frac{\partial^2 v^o}{\partial t^2} \end{aligned} \quad (27)$$

$$\begin{aligned} & \frac{-A_{12}}{R} \left(\frac{\partial u^o}{\partial x} \right) - \frac{A_{22}}{R^2} \left(\frac{\partial v^o}{\partial \theta} + w^o \right) - \frac{A_{26}}{R} \left(\frac{1}{R} \frac{\partial u^o}{\partial \theta} + \frac{\partial v^o}{\partial x} \right) \\ & + B_{11} \left(\frac{\partial^3 u^o}{\partial x^3} \right) + \frac{B_{12}}{R} \left(\frac{\partial^3 v^o}{\partial x^2 \partial \theta} + \frac{2 \partial^2 w^o}{\partial x^2} + \frac{1}{R} \frac{\partial^3 u^o}{\partial \theta^2 \partial x} \right) \end{aligned}$$

$$\begin{aligned}
& + B_{16} \left(\frac{3}{R} \frac{\partial^3 u^o}{\partial x^2 \partial \theta} + \frac{\partial^3 v^o}{\partial x^3} \right) + \frac{B_{22}}{R^3} \left(\frac{\partial v^o}{\partial \theta^3} + \frac{\partial^2 w^o}{\partial \theta^2} \right) \\
& + \frac{B_{26}}{R^2} \left(\frac{1}{R} \frac{\partial^3 u^o}{\partial x \partial \theta^2} + \frac{\partial^3 v^o}{\partial x^2 \partial \theta} \right) - D_{11} \left(\frac{\partial^4 w^o}{\partial x^4} \right) - \frac{2 D_{12}}{R^2} \left(\frac{\partial^2 w^o}{\partial x^2 \partial \theta^2} \right) \\
& - \frac{4 D_{16}}{R} \left(\frac{\partial^4 w^o}{\partial x^3 \partial \theta} \right) - \frac{D_{22}}{R^4} \left(\frac{\partial^4 w^o}{\partial \theta^4} \right) - \frac{4 D_{26}}{R^3} \left(\frac{\partial^4 w^o}{\partial x \partial \theta^3} \right) \\
& - \frac{4 D_{66}}{R^2} \left(\frac{\partial^4 w^o}{\partial x^2 \partial \theta^2} \right) = \rho \frac{\partial^2 w^o}{\partial t^2} \tag{28}
\end{aligned}$$

The problem is reduced to an arch by assuming that there is no variation in the x -direction. This requires that all terms containing $\partial/\partial x$ equal to zero. When this is done the above equations become:

$$\frac{A_{26}}{R^2} \left(\frac{\partial^2 v^o}{\partial \theta^2} + \frac{\partial w^o}{\partial \theta} \right) + \frac{A_{66}}{R} \left(\frac{1}{R} \frac{\partial^2 u^o}{\partial \theta^2} \right) - \frac{B_{26}}{R^3} \left(\frac{\partial^3 w^o}{\partial \theta^3} \right) = \rho \frac{\partial^2 u^o}{\partial t^2} \tag{29}$$

$$\frac{A_{22}}{R^2} \left(\frac{\partial^2 v^o}{\partial \theta^2} + \frac{\partial w^o}{\partial \theta} \right) + \frac{A_{26}}{R} \left(\frac{1}{R} \frac{\partial^2 u^o}{\partial \theta^2} \right) - \frac{B_{22}}{R^3} \left(\frac{\partial^3 w^o}{\partial \theta^3} \right) = \rho \frac{\partial^2 v^o}{\partial t^2} \tag{30}$$

$$\begin{aligned}
& - \frac{A_{22}}{R^2} \left(\frac{\partial v^o}{\partial \theta} + w^o \right) - \frac{A_{26}}{R} \left(\frac{1}{R} \frac{\partial u^o}{\partial \theta} \right) \\
& + \frac{B_{22}}{R^3} \left(\frac{\partial^3 v^o}{\partial \theta^3} + \frac{\partial^2 w^o}{\partial \theta^2} \right) - \frac{D_{22}}{R^4} \left(\frac{\partial^4 w^o}{\partial \theta^4} \right) = \rho \frac{\partial^2 w^o}{\partial t^2} \tag{31}
\end{aligned}$$

The boundary conditions given by Eq. (25) can be satisfied by specifying the displacements and some of the slopes at the ends of the arch, or by specifying that certain forces and moments go to zero at the boundaries. The boundary conditions for a clamped-clamped arch are:

For $\theta = 0$

$$u^o(0, t) = v^o(0, t) = w^o(0, t) = \frac{\partial w^o}{\partial \theta}(0, t) = 0$$

For $\theta = \pi$

$$u^o(\pi, t) = v^o(\pi, t) = w^o(\pi, t) = \frac{\partial w^o}{\partial \theta}(\pi, t) = 0 \quad (32)$$

The physical significance of these boundary conditions are that the displacements and the slope of the arch are specified, and are in fact zero, at both ends. These boundary conditions are sufficient to determine the system as presented. There are other boundary conditions, which involve the x -direction, but they are not relevant to the arch problem. They are relevant when the equations for a shell, Eqs. (26), (27), and (28), are employed.

To simplify the equations further, material symmetries are assumed. An orthotropic or isotropic material has the characteristics of:

$$B_{ij} = A_{16} = A_{26} = D_{16} = D_{26} = 0$$

Removing these terms from the equations of motion yields:

$$\frac{A_{66}}{R} \left(\frac{1}{R} \frac{\partial^2 u^o}{\partial \theta^2} \right) = \rho \frac{\partial^2 u^o}{\partial t^2} \quad (33)$$

$$\frac{A_{22}}{R^2} \left(\frac{\partial^2 v^o}{\partial \theta^2} + \frac{\partial w^o}{\partial \theta} \right) = \rho \frac{\partial^2 v^o}{\partial t^2} \quad (34)$$

$$-\frac{A_{22}}{R^2} \left(\frac{\partial v^o}{\partial \theta} + w^o \right) - \frac{D_{22}}{R^4} \left(\frac{\partial^4 w^o}{\partial \theta^4} \right) = \rho \frac{\partial^2 w^o}{\partial t^2} \quad (35)$$

It should be noted that the first equation is not coupled to the second two, and is merely the classical wave equation with zero displacement at the endpoints. The second and third equations, Eqs. (34) and (35), form the system whose solution is the basis of the rest of this thesis. The boundary conditions for these two equations can be written:

For $\theta = 0$

$$v^o(0, t) = w^o(0, t) = \frac{\partial w^o}{\partial \theta}(0, t) = 0$$

For $\theta = \pi$

$$v^o(\pi, t) = w^o(\pi, t) = \frac{\partial w^o(\pi, t)}{\partial \theta}(\pi, t) = 0 \quad (36)$$

COMPARISONS

Before continuing with the solution of these two coupled partial differential equations, Eqs. (34) and (35), it would be useful to find out how they compare to existing models which describe the same physical system they are supposed to model. To this end, they were compared to other formulations, both from shell theory, [2] and [3], and from papers available in the literature on isotropic arches [5]. The equations obtained here agree exactly with those obtained by Whitney, [2], because the methods of formulation were identical. Comparison with Flugge's equations [3] was a little more difficult, because his was an isotropic formulation for cylinders in bending. It was decided to compare equations for the static case, to see how the order of the equations compared. The results are presented exactly as in his book; only the notation has been changed to facilitate comparisons with the equations presented earlier. From [3]:

$$\frac{\partial^2 u^o}{\partial x^2} + \left(\frac{1 - \nu}{2} \right) \frac{\partial^2 u^o}{\partial \theta^2} - \left(\frac{1 + \nu}{2} \right) \frac{\partial^2 v^o}{\partial x \partial \theta} + \nu \frac{\partial w^o}{\partial x} + \frac{p_x a^2}{D} = 0 \quad (37)$$

$$\frac{1 + \nu}{2} \frac{\partial^2 u^o}{\partial x \partial \theta} + \frac{\partial^2 v^o}{\partial \theta^2} + \frac{1 - \nu}{2} \frac{\partial^2 v^o}{\partial x^2} + \frac{\partial w^o}{\partial \theta} + \frac{p_\theta a^2}{D} = 0 \quad (38)$$

$$\nu \frac{\partial u^o}{\partial x} + \frac{\partial v^o}{\partial \theta} + w + k \left(\frac{\partial^4 w^o}{\partial x^4} + \frac{2 \partial^4 w^o}{\partial x^2 \partial \theta^2} + \frac{\partial^4 w^o}{\partial \theta^4} \right) - \frac{p_r a^2}{D} = 0 \quad (39)$$

Here, ν is Poisson's ratio, and k is another material constant; p_x , p_θ , and p_r are the applied loads in the indicated directions, which are equal to zero. In this comparison, these equations are essentially the same as Eqs. (29)-(31) when isotropic conditions are imposed, which is to say $A_{16} = A_{26} = D_{16} = D_{26} = 0$, $B_{ij} = 0$, $A_{11} = A_{22}$, and $D_{11} = D_{22}$

Comparison with an isotropic formulation for an arch is a little more difficult because the assumptions made at the beginning of the formulation were different than those made here. However, it is necessary for completeness to present the equations which generated the isotropic results used for comparison later. Again, the notation has been changed so that it is consistent with that used in the earlier equations. From Archer [5]:

$$\frac{EI}{R^4} \left(\frac{\partial^6 v^o}{\partial \theta^6} + 2 \frac{\partial^4 v^o}{\partial \theta^4} + \frac{\partial^2 v^o}{\partial \theta^2} \right) = \rho \frac{\partial^2}{\partial t^2} \left(v^o - \frac{\partial^2 v^o}{\partial \theta^2} \right) + K \frac{\partial}{\partial t} \left(v^o - \frac{\partial^2 v^o}{\partial \theta^2} \right) \quad (40)$$

$$w^o = \frac{\partial v^o}{\partial \theta} \quad (41)$$

To attempt a comparison, the relationship $w^o = \partial v^o / \partial \theta$ may be substituted into Eqs. (34) and (35), to give:

$$\frac{A_{22}}{R^2} \left(\frac{\partial^2 v^o}{\partial \theta^2} + \frac{\partial^2 v^o}{\partial \theta^2} \right) = \rho \frac{\partial^2 v^o}{\partial t^2} \quad (42)$$

$$-\frac{A_{22}}{R^2} \left(\frac{\partial v^o}{\partial \theta} + \frac{\partial v^o}{\partial \theta} \right) - \frac{D_{22}}{R^4} \left(\frac{\partial^5 v^o}{\partial \theta^5} \right) = \rho \frac{\partial^3 v^o}{\partial t^2 \partial \theta} \quad (43)$$

These equations can be combined into one, which is:

$$2 \frac{A_{22}}{R^2} \left(\frac{\partial^2 v^o}{\partial \theta^2} + \frac{\partial v^o}{\partial \theta} \right) + \frac{D_{22}}{R^4} \left(\frac{\partial^5 v^o}{\partial \theta^5} \right) = \rho \frac{\partial^2}{\partial t^2} \left(v^o - \frac{\partial v^o}{\partial \theta} \right) \quad (44)$$

The form of this equation is similar to that of Eq. (40), with the most noticeable difference being the order of differentiation, which is one order lower in the shell formulation. Eq. (44) was obtained from a modified beam theory, which could explain part of the difference. As stated before,

the main problem in comparing the two equations is the different assumptions made early in the formulation. Archer [5] assumes inextensibility, Eq. (41) , where the shell theory is based on the Kirchoff-Love hypothesis, and the two are not compatible. However, the results obtained with these different formulations are compared in Chapter 4 and turn out to be surprisingly similar.

The problem, as stated, is to explore the behavior of the system subject to a harmonic forcing function, $F(t) = A e^{i\Omega t}$ where $A = 1$, where the excitation is applied in the tangential direction, at the end $\theta = 0$. The technique chosen to solve the equations of motion was separation of variables, with the time part of the displacement chosen to be a harmonic function. The displacements are written as:

$$w^o(\theta, t) = \tilde{w}(\theta) T(t) \quad (45)$$

$$v^o(\theta, t) = \tilde{v}(\theta) T(t) \quad (46)$$

where $T(t) = e^{i\tilde{\omega}t}$ and $\tilde{\omega}$ = frequency

In order to produce dimensionless equations, the dimensionless displacements, $w = \tilde{w}/h$ and $v = \tilde{v}/h$ are introduced. Eqs. (34) and (35) are non-dimensionalized by dividing by E_θ , the modulus of elasticity in the tangential direction, and multiplying by the radius R . This results in a non-dimensional frequency $\omega = \rho\tilde{\omega}/E_\theta$, where ρ is the mass per unit length of the arch. Taking appropriate derivatives, substituting them into the equations of motion, and canceling the common term $e^{i\omega t}$ leaves:

$$\alpha_{11} \frac{\partial^4 w}{\partial \theta^4} + \alpha_{12} w + \beta_{11} \frac{\partial v}{\partial \theta} = 0 \quad (47)$$

$$\beta_{21} \frac{\partial^2 v}{\partial \theta^2} + \beta_{22} v + \alpha_{21} \frac{\partial w}{\partial \theta} = 0 \quad (48)$$

where

$$\alpha_{11} = \frac{D_{22}}{R^3 E_\theta}, \quad \alpha_{12} = \frac{1}{E_\theta} \left(\frac{A_{22}}{R} - \rho \omega^2 R \right), \quad \alpha_{21} = \frac{A_{22}}{R E_\theta}$$

$$\beta_{11} = \frac{A_{22}}{R E_\theta}, \quad \beta_{21} = \frac{A_{22}}{R E_\theta}, \quad \beta_{22} = \frac{\rho \omega^2 R}{E_\theta} \quad (49)$$

The boundary conditions, again, are homogeneous, i.e.:

For $\theta = 0$

$$v(0) = w(0) = \frac{\partial w(0)}{\partial \theta} = 0 \quad (50)$$

For $\theta = \pi$

$$v(\pi) = w(\pi) = \frac{\partial w(\pi)}{\partial \theta} = 0 \quad (51)$$

Chapter 3

SOLUTION TECHNIQUES

The problem is now to solve two coupled ordinary differential equations, Eqs. (47) and (48). Three methods of solution were explored: Laplace transformations, the method of particular solutions, and eigensolutions. The results for all three are shown and compared. The eigensolution is the most efficient in terms of computer time and is the easiest to modify, should it be desired to explore a higher order theory. It is the eigensolution which was used to generate the results presented for the more complicated case of forced response. All three methods give the same general results, which provides a good check of the solution, and implies that the solution obtained is correct.

Laplace Transformations

The Laplace transform provides a very tidy and elegant solution to the problem. It is the only method which is, without question, a closed-form solution. However, it proved to be a bit unwieldy to program, with problems occurring in the numerical stability of the solution, program

length and run time, and difficulty in applying modifications to the original problem. The Laplace transform provides an excellent solution on paper, but it was difficult to implement.

The Laplace transform of a function is defined as:

$$\bar{w}(s) \equiv \int_0^{\infty} w(\theta) e^{-s\theta} d\theta \quad (52)$$

In practice, tables of transforms are generally used. One very important relationship between a function and its representation in the Laplace domain is the transform of its derivative. The Laplace transform of the n th derivative of a function is defined:

$$\mathcal{L}\left[\frac{d^n w(\theta)}{d\theta^n}\right] = s^n \bar{w}(s) - s^{n-1} w(0) - -s^{n-2} \frac{dw(0)}{d\theta} \dots s \frac{d^{n-2} w(0)}{d\theta^{n-2}} - \frac{d^{n-1} w(0)}{d\theta^{n-1}} \quad (53)$$

where s is the Laplace variable and $\bar{w}(s)$ is the transform of the function $w(\theta)$.

Taking the Laplace transform of both sides of Eqs. (47) and (48) creates a set of equations in matrix form in the Laplace domain. Note that some of the terms obtained in the transformation process are equal to zero due to the boundary conditions at $\theta = 0$, and that only the nonzero terms are shown here.

$$[\tilde{G}(s)] \begin{bmatrix} \bar{w}(s) \\ \bar{v}(s) \end{bmatrix} = [F(s)] \begin{bmatrix} C_1 \\ C_2 \\ C_3 \end{bmatrix} \quad (54)$$

where

$$[\tilde{G}] = \begin{bmatrix} (\alpha_{11} s^4 + \alpha_{12}) & \beta_{11} s \\ \alpha_{21} s & (\beta_{21} s^2 + \beta_{22}) \end{bmatrix} \quad (55)$$

$$[F(s)] = \begin{bmatrix} 0 & (\alpha_{11} s) & \alpha_{11} \\ \beta_{21} & 0 & 0 \end{bmatrix} \quad (56)$$

$$\begin{bmatrix} C_1 \\ C_2 \\ C_3 \end{bmatrix} = \begin{bmatrix} \frac{dv}{d\theta} \\ \frac{d^2w}{d\theta^2} \\ \frac{d^3w}{d\theta^3} \end{bmatrix} \quad (57)$$

In order to isolate the \bar{w} and \bar{v} terms, it is necessary to invert the coefficient matrix $[\tilde{G}]$. Because $[\tilde{G}]^{-1} = \frac{1}{g(s)} [G]$, the equations of motion in the Laplace domain can now be written:

$$\begin{bmatrix} \bar{w}(s) \\ \bar{v}(s) \end{bmatrix} = \frac{1}{g(s)} [G(s)] [F(s)] \begin{bmatrix} C_1 \\ C_2 \\ C_3 \end{bmatrix} \quad (58)$$

where

$$[G(s)] = \begin{bmatrix} (\beta_{21} s^2 + \beta_{22}) & -\beta_{11} s \\ -\alpha_{21} s & (\alpha_{11} s^4 + \alpha_{12}) \end{bmatrix} \quad (59)$$

$$g(s) = \alpha_{11} \beta_{21} s^6 + \alpha_{11} \beta_{22} s^4 + (\alpha_{13} \beta_{21} - \alpha_{21} \beta_{11}) s^2 + \alpha_{12} \beta_{22} \quad (60)$$

These equations can now be solved to give an expression for w and v by taking the inverse Laplace transformation of the Eq. (58). This results in a set of equations with a total of three unknowns, $[C_1 \ C_2 \ C_3]^T$

$$\begin{bmatrix} w(\theta) \\ v(\theta) \end{bmatrix} = [\tilde{F}(\theta)] \begin{bmatrix} C_1 \\ C_2 \\ C_3 \end{bmatrix} \quad (61)$$

where

$$[\tilde{F}(\theta)] = \mathcal{L}^{-1} \left\{ \frac{1}{g(s)} [G(s)] [F(s)] \right\} \quad (62)$$

The boundary conditions at $\theta = \pi$ are given in Eq. (51). When these conditions are applied, the resulting system is:

$$\begin{bmatrix} v(\pi) \\ w(\pi) \\ \frac{dw(\pi)}{d\theta} \end{bmatrix} = [H(\pi)] \begin{bmatrix} C_1 \\ C_2 \\ C_3 \end{bmatrix} = \begin{bmatrix} 0 \\ 0 \\ 0 \end{bmatrix} \quad (63)$$

where

$$[H(\theta)] = \begin{bmatrix} \tilde{f}_{21}(\theta) & \tilde{f}_{22}(\theta) & \tilde{f}_{23}(\theta) \\ \tilde{f}_{11}(\theta) & \tilde{f}_{12}(\theta) & \tilde{f}_{13}(\theta) \\ \tilde{f}_{11}'(\theta) & \tilde{f}_{12}'(\theta) & \tilde{f}_{13}'(\theta) \end{bmatrix} \quad (64)$$

To get a non-trivial solution for the unknown constants, $v'(0)$, $w''(0)$, and $w'''(0)$, the determinant of $[H(\theta)]$ must equal zero. Because all the elements of $[H(\theta)]$ contain ω^2 in some form, it was decided to iterate for the values of ω^2 that yield a zero determinant. It was at this point that the technique encountered problems, and other alternatives were considered.

The Method of Particular Solutions

The next solution is the method of particular solutions, as proposed by A. Miele, [6]. The problem as presented is a linear, two-point boundary-value problem so this method is appropriate. The technique involves numerical integration, and thus is not a closed-form solution, nor is it as elegant as the Laplace transform. However, its accuracy is limited only by that of the integration, and the results were comparable to those for the transform technique. The solution presented here is just for the given problem; those wishing to see the general solution are referred to Miele's paper.

The first step in this solution is to perform a reduction of order on the system of equations, to change from two equations, fourth and second order respectively, to a system of six first order equations, known as a state-vector approach. Starting from Eqs. (47) and (48), let

$y_1 = w$, and $y_2 = v$. After performing standard substitutions in reduction of order, the resulting system of equations has the form:

$$y_1' = y_3 \quad y_2' = y_4 \quad y_3' = y_5$$

$$y_4' = -\frac{\beta_{22}}{\beta_{21}} y_2 - \frac{\alpha_{21}}{\beta_{21}} y_3 \quad y_5' = y_6 \quad y_6' = -\frac{\alpha_{12}}{\alpha_{11}} y_1 - \frac{\beta_{12}}{\alpha_{11}} y_4 \quad (65)$$

where $y' \equiv \frac{dy}{d\theta}$

$$y_1 = w, \quad y_2 = v, \quad y_3 = \frac{\partial w}{\partial \theta},$$

$$y_4 = \frac{\partial v}{\partial \theta}, \quad y_5 = \frac{\partial^2 w}{\partial \theta^2}, \quad y_6 = \frac{\partial^3 w}{\partial \theta^3}. \quad (66)$$

Writing this in matrix form:

$$\begin{bmatrix} y_1 \\ y_2 \\ y_3 \\ y_4 \\ y_5 \\ y_6 \end{bmatrix}' = \begin{bmatrix} 0 & 0 & 1 & 0 & 0 & 0 \\ 0 & 0 & 0 & 1 & 0 & 0 \\ 0 & -\frac{\beta_{22}}{\beta_{21}} & 0 & 0 & 1 & 0 \\ 0 & 0 & -\frac{\alpha_{21}}{\beta_{21}} & 0 & 0 & 0 \\ 0 & 0 & 0 & 0 & 0 & 1 \\ -\frac{\alpha_{12}}{\alpha_{11}} & 0 & 0 & -\frac{\beta_{12}}{\alpha_{11}} & 0 & 0 \end{bmatrix} \begin{bmatrix} y_1 \\ y_2 \\ y_3 \\ y_4 \\ y_5 \\ y_6 \end{bmatrix} \quad (67)$$

It follows from Eq. (49), $\alpha_{21}/\beta_{21} \equiv 1$

Eq. (67) can be written in the form:

$$[y]' = [A][y] \quad (68)$$

Matrix $[A]$ is the same as the one in Eq. (67), and is note the extensional matrix $[A]$ defined in Eq. (9). The boundary conditions in this notation are:

$$y_1(0) = y_1(\pi) = y_2(0) = y_2(\pi) = y_3(0) = y_3(\pi) = 0 \quad (69)$$

The problem statement for the method of particular solutions is as follows:

$$[y]' = [A][y] + [\alpha] \quad (70)$$

$$[B][y(0)] = [\beta] \quad (71)$$

$$[C][y(\pi)] = [\gamma] \quad (72)$$

where

$$[B] = [C] = \begin{bmatrix} 1 & 0 & 0 & 0 & 0 & 0 \\ 0 & 1 & 0 & 0 & 0 & 0 \\ 0 & 0 & 1 & 0 & 0 & 0 \end{bmatrix} \quad (73)$$

$$[\beta] = [\gamma] = \begin{bmatrix} 0 \\ 0 \\ 0 \end{bmatrix}, \quad (74)$$

Given an n th order system with p given initial conditions, when employing this solution technique it is necessary to integrate $q = n - p + 1$ times. In this case the system is sixth order, with three proscribed initial conditions. Therefore, the solution is obtained by integrating from 0 to π four times, each time with different initial conditions. Let $[\tilde{y}]_i$ be a solution obtained by the i th integration. Then $[\tilde{y}(0)]_i$ is the corresponding initial condition used for that integration. The set $[\tilde{y}(0)]_i$, $i = 1, 2, 3, 4$, must satisfy the required boundary conditions given by Eq. (69), so they must be chosen so that the first three elements are zero. Choosing the easiest linearly independent set of boundary conditions that meet this requirement gives:

$$[\tilde{y}(0)]_1 = \begin{bmatrix} 0 \\ 0 \\ 0 \\ 1 \\ 0 \\ 0 \end{bmatrix}, \quad [\tilde{y}(0)]_2 = \begin{bmatrix} 0 \\ 0 \\ 0 \\ 0 \\ 1 \\ 0 \end{bmatrix}, \quad [\tilde{y}(0)]_3 = \begin{bmatrix} 0 \\ 0 \\ 0 \\ 0 \\ 0 \\ 1 \end{bmatrix}, \quad [\tilde{y}(0)]_4 = \begin{bmatrix} 0 \\ 0 \\ 0 \\ 0 \\ 0 \\ 0 \end{bmatrix} \quad (75)$$

Numerically integrating four times from 0 to π , once each with the boundary conditions $[\tilde{y}(0)]_i$, gives four linearly independent solutions for the proscribed system, denoted $[\tilde{y}]_i$. The actual solution to the system is a linear combination of these solutions, which can be written as:

$$[y] = \sum_{i=1}^4 C_i [\tilde{y}]_i \quad (76)$$

The unknown constants C_i can be determined by applying the boundary conditions at π in conjunction with the auxiliary equation

$$\sum_{i=1}^4 C_i = 1 \quad (77)$$

This may be expressed as:

$$y_j(\pi) = \sum_{i=1}^4 C_i [\tilde{y}_j]_i \quad (78)$$

where $[\tilde{y}_j]_i$ is the j th element of the vector $[\tilde{y}]_i = \tilde{y}_{ij}$

Because all of the elements of the proscribed boundary conditions happen to be zero, the resulting set of equations are:

$$\begin{bmatrix} y_1(\pi) \\ y_2(\pi) \\ y_3(\pi) \end{bmatrix} = \begin{bmatrix} \tilde{y}_{11} & \tilde{y}_{21} & \tilde{y}_{31} & \tilde{y}_{41} \\ \tilde{y}_{12} & \tilde{y}_{22} & \tilde{y}_{32} & \tilde{y}_{42} \\ \tilde{y}_{13} & \tilde{y}_{23} & \tilde{y}_{33} & \tilde{y}_{43} \end{bmatrix} \begin{bmatrix} C_1 \\ C_2 \\ C_3 \\ C_4 \end{bmatrix} = \begin{bmatrix} 0 \\ 0 \\ 0 \end{bmatrix} \quad (79)$$

Applying the auxiliary equation yields a the set of equations:

$$\begin{bmatrix} \tilde{y}_{11} & \tilde{y}_{21} & \tilde{y}_{31} & \tilde{y}_{41} \\ \tilde{y}_{12} & \tilde{y}_{22} & \tilde{y}_{32} & \tilde{y}_{42} \\ \tilde{y}_{13} & \tilde{y}_{23} & \tilde{y}_{33} & \tilde{y}_{43} \\ 1 & 1 & 1 & 1 \end{bmatrix} \begin{bmatrix} C_1 \\ C_2 \\ C_3 \\ C_4 \end{bmatrix} = \begin{bmatrix} 0 \\ 0 \\ 0 \\ 1 \end{bmatrix} \quad (80)$$

However, application of this solution to the given system was more complicated than simply solving a four by four system of equations. The fourth initial condition $[\tilde{y}(0)]_4$ is identically equal to zero, and yields a zero solution at $\theta = \pi$. This implies that

$$[\tilde{y}]_4 \equiv [0 \ 0 \ 0 \ 0 \ 0 \ 0]^T$$

and thus C_4 is completely arbitrary and adds nothing to the solution. Therefore, it is chosen to be zero and is dropped from the solution [7]. Reworking the problem with only three integrations yields the same first three solutions as before, and the system can be written:

$$\begin{bmatrix} \tilde{y}_{11} & \tilde{y}_{21} & \tilde{y}_{31} \\ \tilde{y}_{12} & \tilde{y}_{22} & \tilde{y}_{32} \\ \tilde{y}_{13} & \tilde{y}_{23} & \tilde{y}_{33} \end{bmatrix} \begin{bmatrix} C_1 \\ C_2 \\ C_3 \end{bmatrix} = \begin{bmatrix} 0 \\ 0 \\ 0 \end{bmatrix} \quad (81)$$

and

$$C_1 + C_2 + C_3 = 1: \quad (82)$$

The last equation, Eq. (82), essentially defines the length of the solution vector, while the three by three system defines that same arrangement as in the Laplace section. That is to say, the determinant of the coefficient matrix must be equal to zero to yield a non-trivial solution for the C_i . This is done again by iterating for the value of ω that yields a zero determinant. The solution given by this method was accurate to the accuracy of the numerical integration, but numerical problems occurred before achieving a sufficiently small determinant.

Eigensolution

The solution begins the same way as the method of particular solutions. However, starting from Eq. (68):

$$[y]' = [A][y]$$

the solutions differ.

This is a sixth order equation, so the matrix $[A]$ has six eigenvalues, and six associated eigenvectors. The general form of the solution is assumed to be [8]:

$$[y] = \sum_{i=1}^6 C_i [\zeta]_i e^{\lambda_i \theta} \quad (83)$$

where λ_i are the eigenvalues of $[A]$, and $[\zeta]_i$ are the corresponding eigenvectors.

There are arguments for and against classification of this approach as a closed-form solution. Because the eigenvalues and eigenvectors were found numerically, it is probably not an exact solution in this instance. However, this technique allowed the determinant to come much closer to zero before becoming unstable due to numerical problems.

Once the solution is found, the six boundary conditions can be applied. For ease of notation, let ζ_{ij} equal the j th element of the i th eigenvector. Then applying the boundary conditions results in the system:

$$\begin{bmatrix} y_1(0) \\ y_2(0) \\ y_3(0) \\ y_1(\pi) \\ y_2(\pi) \\ y_3(\pi) \end{bmatrix} = \begin{bmatrix} \zeta_{11} & \zeta_{21} & \zeta_{31} & \zeta_{41} & \zeta_{51} & \zeta_{61} \\ \zeta_{12} & \zeta_{22} & \zeta_{32} & \zeta_{42} & \zeta_{52} & \zeta_{62} \\ \zeta_{13} & \zeta_{23} & \zeta_{33} & \zeta_{43} & \zeta_{53} & \zeta_{63} \\ \zeta_{11} e^{\lambda_1 \pi} & \zeta_{21} e^{\lambda_2 \pi} & \zeta_{31} e^{\lambda_3 \pi} & \zeta_{41} e^{\lambda_4 \pi} & \zeta_{51} e^{\lambda_5 \pi} & \zeta_{61} e^{\lambda_6 \pi} \\ \zeta_{12} e^{\lambda_1 \pi} & \zeta_{22} e^{\lambda_2 \pi} & \zeta_{32} e^{\lambda_3 \pi} & \zeta_{42} e^{\lambda_4 \pi} & \zeta_{52} e^{\lambda_5 \pi} & \zeta_{62} e^{\lambda_6 \pi} \\ \zeta_{13} e^{\lambda_1 \pi} & \zeta_{23} e^{\lambda_2 \pi} & \zeta_{33} e^{\lambda_3 \pi} & \zeta_{43} e^{\lambda_4 \pi} & \zeta_{53} e^{\lambda_5 \pi} & \zeta_{63} e^{\lambda_6 \pi} \end{bmatrix} \begin{bmatrix} C_1 \\ C_2 \\ C_3 \\ C_4 \\ C_5 \\ C_6 \end{bmatrix} = \begin{bmatrix} 0 \\ 0 \\ 0 \\ 0 \\ 0 \\ 0 \end{bmatrix} \quad (84)$$

Again, the determinant of a matrix must be zero to yield a non-trivial solution for the unknown constants.

Comparison of Results

All three methods gave the same solution to five figures, and these results are presented in Table (1).

The eigensolution was clearly superior to both other methods in efficiency and numerical stability, that is, it does not become significantly less stable at the higher frequencies as do the other solutions. It was therefore chosen as the method of solution for all the loading cases considered in the next section.

Comparison of Frequencies

There are two readily available sources for comparison for the acceptability of the computed natural frequencies - Archer [5] which is a theoretical model of an isotropic arch, and experimental data acquired by Collins, [9]. Unfortunately, Collins' work was done on arches with complicated cross-sections, an I-section and a channel section, and this model of a composite arch cannot, at this time, incorporate the extra factors necessary to model such arches. To give some basis for comparison, it was decided to simply normalize all predicted and observed frequencies by their

Table 1. Eigensolution

n	omega (rad/sec)
1	44.3237
2	93.1525
3	168.035
4	253.548
5	364.188
6	481.657

fundamental frequency. The results of this comparison are shown in Fig. (3) and Table (2). The arch used in this model is indicated by the caption 'composite' and Archer's model by the caption 'isotropic'.

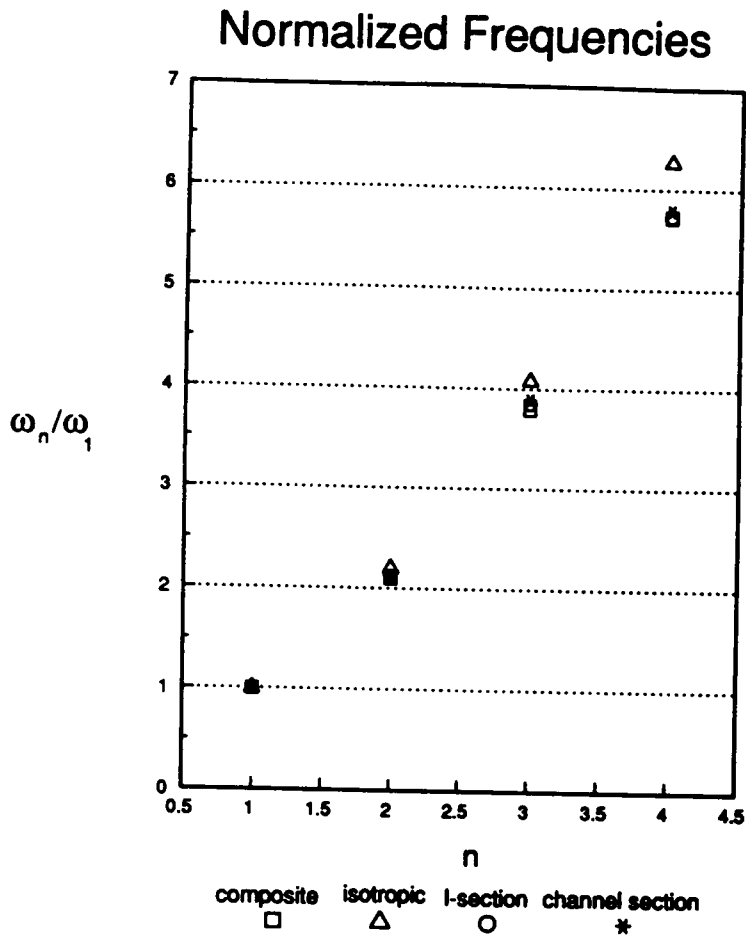


Figure 3. Comparison of normalized frequencies: normalized frequencies predicted by the isotropic and composite models and normalized frequencies observed on the I-section and channel section arches

Table 2. Normalized Frequencies

n	composite	isotropic	I-section	Channel
2	2.10	2.20	2.12	2.11
3	3.79	4.08	3.85	3.89
4	5.72	6.27	5.73	5.79

Chapter 4

RESULTS

Free Vibrations

Once a suitable solution technique was found, the mode shapes could be determined. In Eq. (84), the last constant, C_6 , was set equal to one, and the last equation from the matrix was dropped. Then, the rest of the constants can be determined in terms of C_6 i.e.

$$\begin{bmatrix} \zeta_{11} & \zeta_{21} & \zeta_{31} & \zeta_{41} & \zeta_{51} \\ \zeta_{12} & \zeta_{22} & \zeta_{32} & \zeta_{42} & \zeta_{52} \\ \zeta_{13} & \zeta_{23} & \zeta_{33} & \zeta_{43} & \zeta_{53} \\ \zeta_{11} e^{\lambda_1 \pi} & \zeta_{21} e^{\lambda_2 \pi} & \zeta_{31} e^{\lambda_3 \pi} & \zeta_{41} e^{\lambda_4 \pi} & \zeta_{51} e^{\lambda_5 \pi} \\ \zeta_{12} e^{\lambda_1 \pi} & \zeta_{22} e^{\lambda_2 \pi} & \zeta_{32} e^{\lambda_3 \pi} & \zeta_{42} e^{\lambda_4 \pi} & \zeta_{52} e^{\lambda_5 \pi} \end{bmatrix} \begin{bmatrix} C_1 \\ C_2 \\ C_3 \\ C_4 \\ C_5 \end{bmatrix} = - \begin{bmatrix} \zeta_{61} \\ \zeta_{62} \\ \zeta_{63} \\ \zeta_{61} e^{\lambda_6 \pi} \\ \zeta_{62} e^{\lambda_6 \pi} \end{bmatrix} \quad (85)$$

This is the form $[A] \{c\} = \{b\}$ and can be solved by standard means, such as Gaussian elimination. Now, with the constants determined as

$$[C_1 \ C_2 \ C_3 \ C_4 \ C_5 \ 1]^T \tag{86}$$

the solution for the displacements is completed by inserting these constants into Eq. (83):

$$[y] = \sum_{i=1}^6 C_i [\zeta]_i e^{\lambda_i \theta}$$

The graphs of v , w , and w' are shown in Figs. (4), (6), and (8). For comparison, the graphs for the same variables as computed by Archer [5] with an isotropic model are shown in Figs. (5), (7), and (9), where $\phi = v$, $\phi' = w$, and $\phi'' = w'$. Note that some of the graphs are the negative of the ones in Archer's paper - this is a manifestation of the nature of a vibration where the motion of a particular point is described by an oscillation between $\pm \Delta$. Some of the graphs are of the position at $-\Delta$ rather than at $+\Delta$, but are valid representations of the mode shape.

Going back to the state vector formulation and recalling that $y_1 = w$, and $y_2 = v$ the complete displacement of any point θ on the arch can be determined by combining the radial, w , and tangential, v , displacements. These mode shapes are shown in Figs. (10) and (11). The tangential displacement contributes significantly only to the first mode, which is a swaying type motion. The rest of the modes are mostly radial in nature, and these modes are confirmed both by the isotropic model, Fig. (12), and by experimental data, as can be seen by Fig. (13).

FORCED RESPONSE

The arch was excited by an applied displacement at the $\theta = 0$ end, as illustrated in Fig. (14). The method for solving for the forced response was chosen to be the frequency response function. This involves applying an excitation of $v(0) = A e^{i\Omega t}$, $A = 1$, and finding the response to that for an extensive range of Ω . Given a forcing function, it is possible to obtain its Fourier components,

$$\Omega = \Omega_1$$

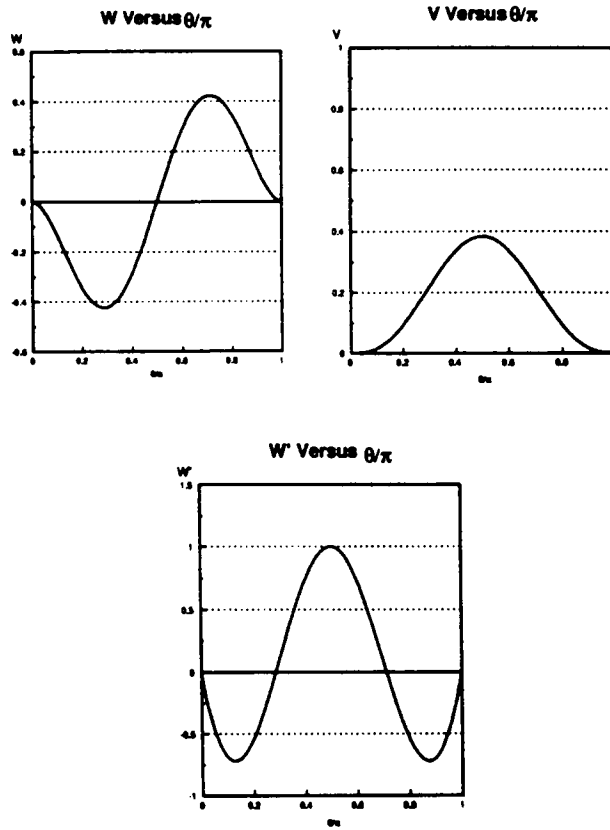
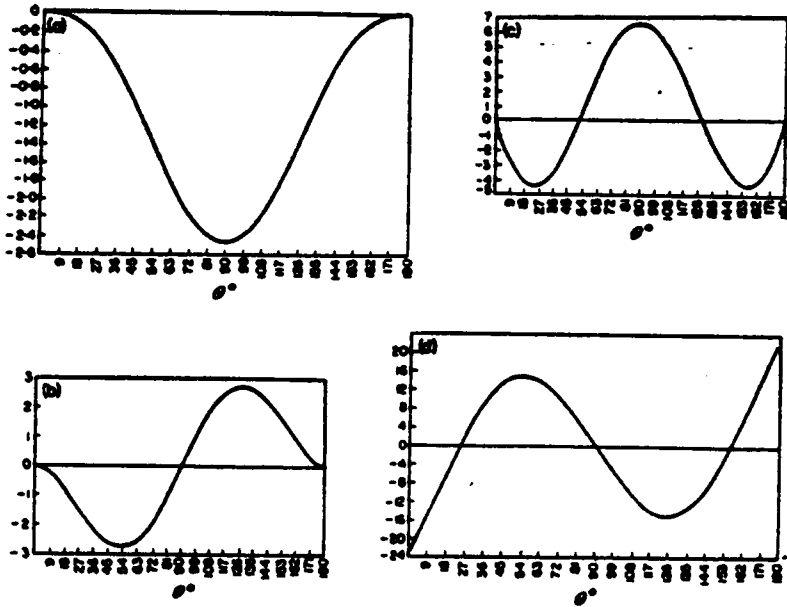


Figure 4. v , w , and w' versus theta, composite: tangential and radial displacements, and slope of arch for the first natural frequency using the composite model



Graph of (a) φ_1 , (b) φ_1' , (c) φ_1'' , (d) φ_1''' .

Figure 5. v , w , and w' versus theta, isotropic: tangential and radial displacements, and slope of arch for the first natural frequency using the isotropic model

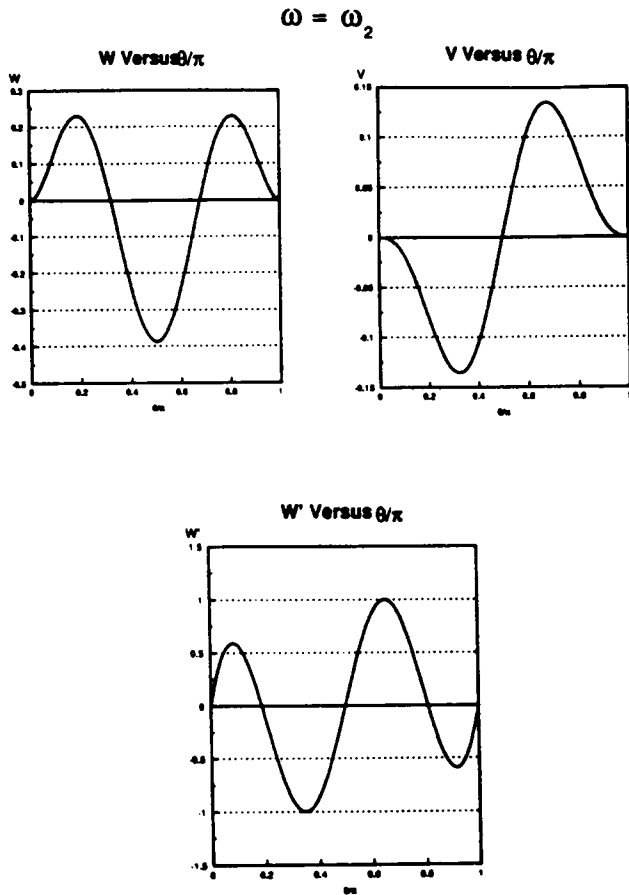


Figure 6. v , w , and w' versus theta, composite: tangential and radial displacements, and slope of arch for the second natural frequency using the composite model

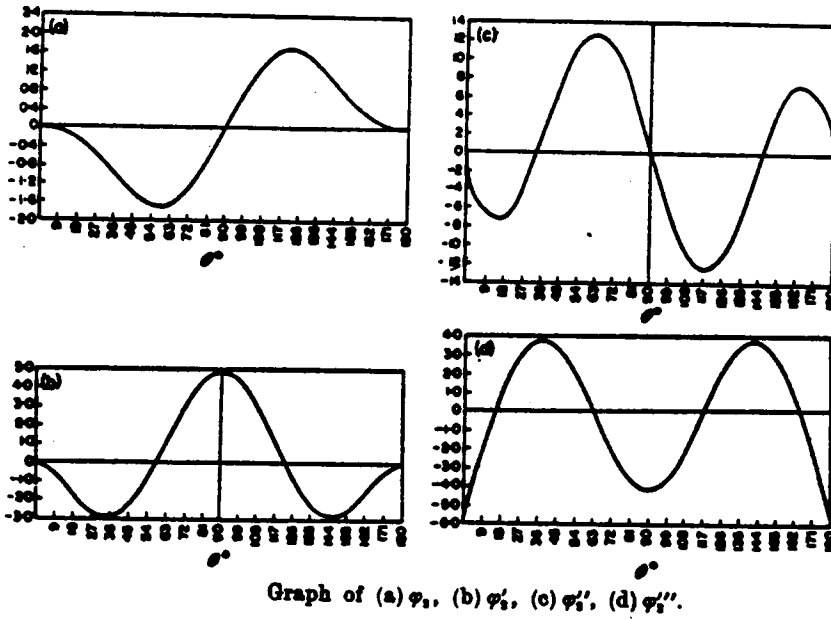


Figure 7. v , w , and w' versus theta, isotropic: tangential and radial displacements, and slope of arch for the second natural frequency using the isotropic model

$$\Omega = \Omega_3$$

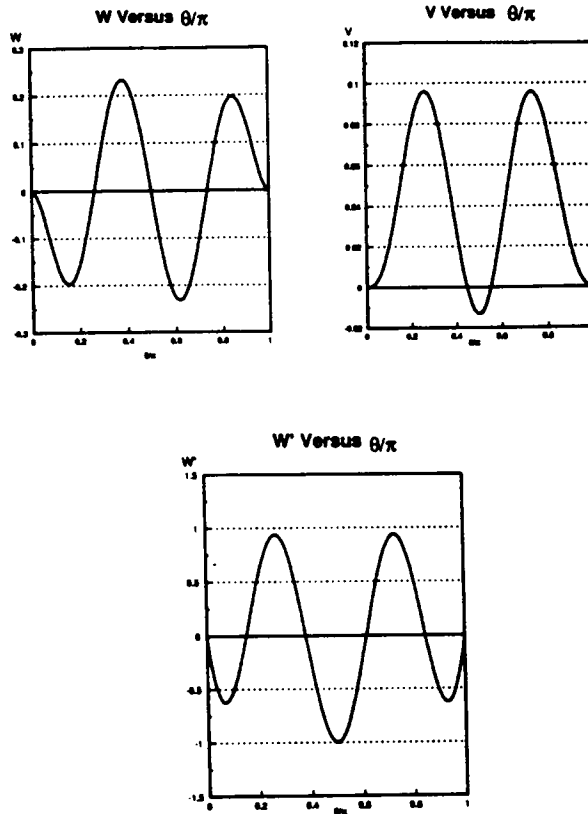
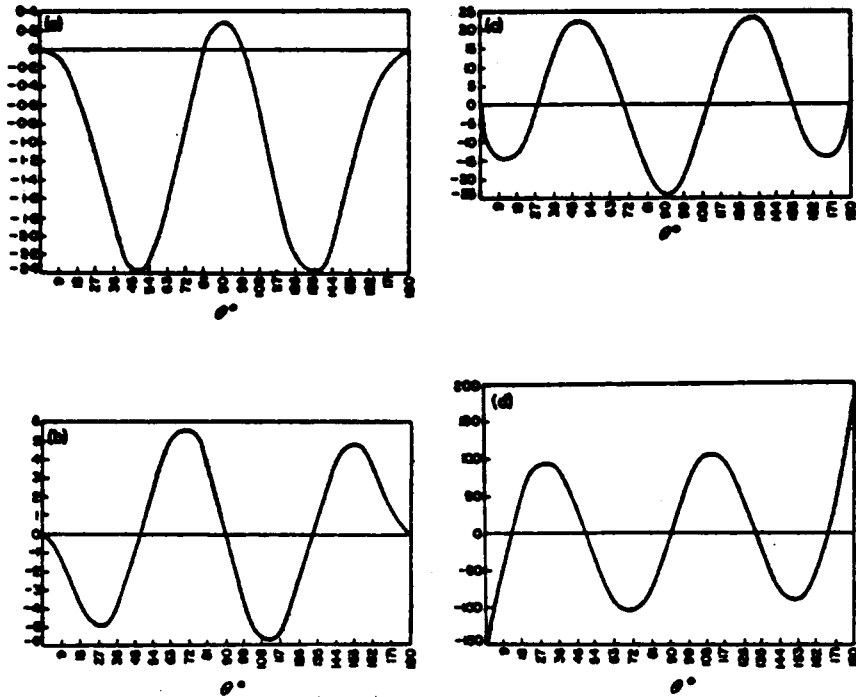


Figure 8. v , w , and w' versus theta, composite: tangential and radial displacements, and slope of arch for the third natural frequency using the composite model



Graph of (a) φ_s , (b) φ'_s , (c) φ''_s , (d) φ'''_s .

Figure 9. v , w , and w' versus theta, isotropic: tangential and radial displacements, and slope of arch for the third natural frequency using the isotropic model

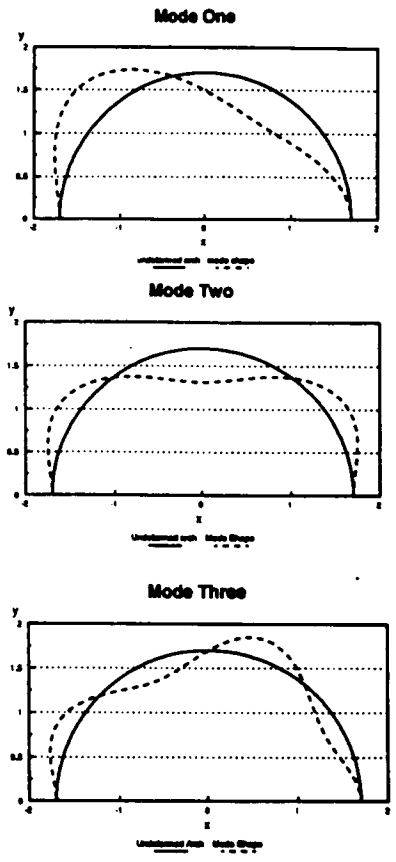


Figure 10. Total displacement: mode shapes of arch for the first three natural frequencies using the composite model

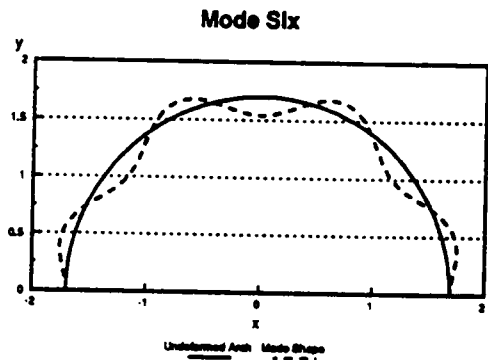
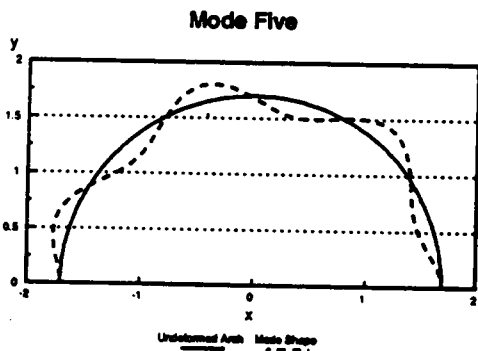
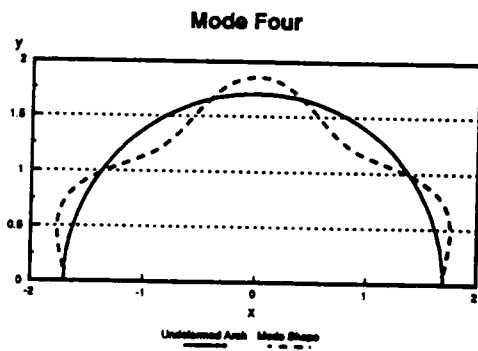


Figure 11. Total displacement: mode shapes of arch for the second three natural frequencies using the composite model

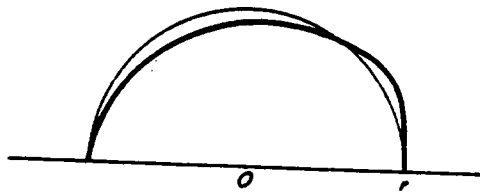


Fig. A-5. Sketch of first (fundamental) mode of vibration.

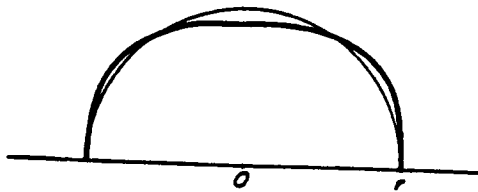


Fig. A-6. Sketch of second mode of vibration.

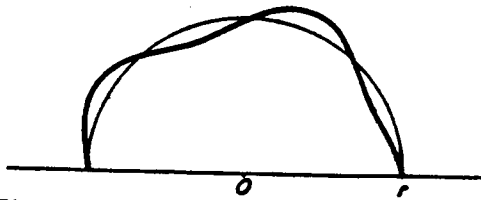


Fig. A-7. Sketch of third mode of vibration.

Figure 12. Total displacement: mode shapes of arch for the first three natural frequencies using the isotropic model

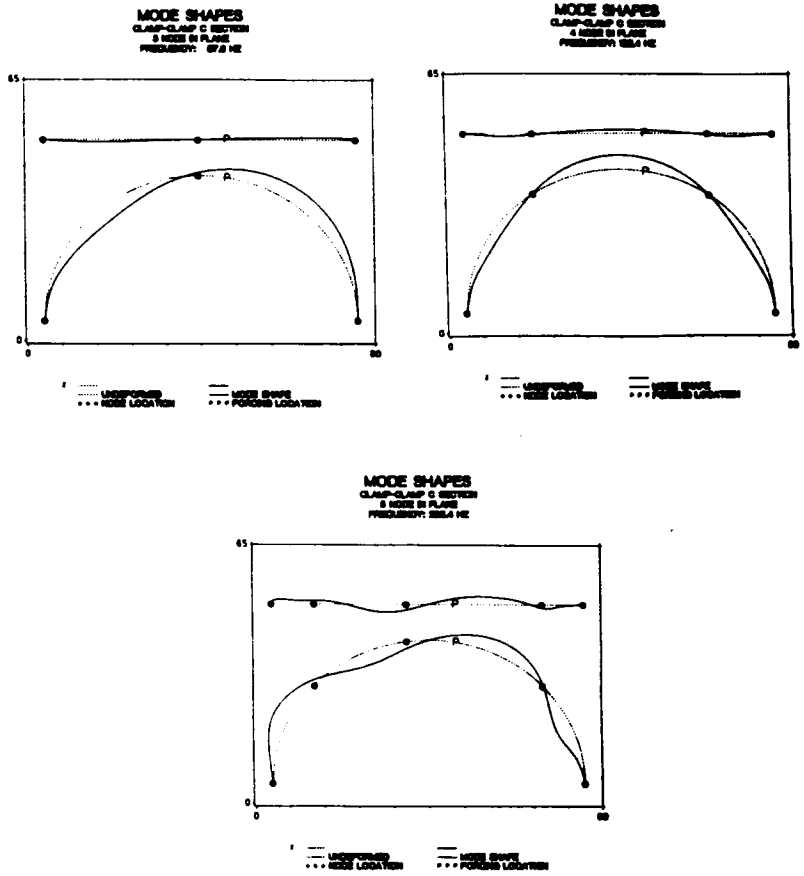


Figure 13. Total displacement: mode shapes of arch for the first three natural frequencies using experimental data

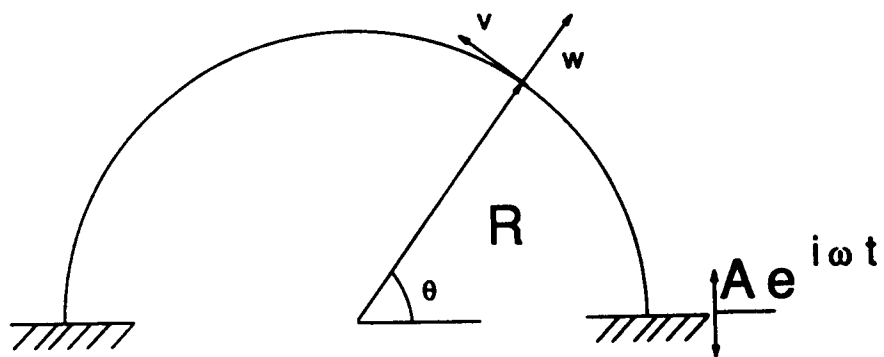


Figure 14. Arch: subject to an excitation at $\theta = 0$

and the complete response can be found by multiplying the frequency response function by those Fourier components and taking the inverse Fourier transform of the product.

Frequency Response Function

The problem is now one of inhomogeneous boundary conditions, that is, the excitation in this model enters into the equations through the boundary conditions, i.e., the value of $v(0) = A e^{i\Omega t}$, $A = 1$, rather than $v(0) = 0$. For ease of calculation, the excitation is included in the equations of motion, rather than in the boundary conditions. To introduce the excitation into the equations of motion, and to render the boundary conditions homogeneous, it is necessary to make a change of variables, from v , the actual tangential displacement, to V , the relative tangential displacement defined:

$$V(r, \theta, t) = v - \left(\frac{\pi - \theta}{\pi} \right) e^{i\Omega t} \quad (87)$$

Note that at $\theta = \pi$, V and v are identical. The displacements are assumed to be of a form:

$$w(\theta, t) = \tilde{w}(\theta) e^{i\Omega t} \quad \text{and} \quad V(\theta, t) = \tilde{v}(\theta) e^{i\Omega t} \quad (88)$$

Non-dimensionalizing as in the free vibration section, the equations of motions for the forced response problem are

$$\alpha_{11} \frac{\partial^4 w}{\partial \theta^4} + \alpha_{12} w + \beta_{11} \frac{\partial v}{\partial \theta} = \mu_1 \quad (89)$$

$$\beta_{21} \frac{\partial^2 v}{\partial \theta^2} + \beta_{22} v + \alpha_{21} \frac{\partial w}{\partial \theta} = \mu_2 \quad (90)$$

where the constants are the same as defined in Eq. (49) except :

$$\alpha_{12} = \frac{1}{E_\theta} \left(\frac{A_{22}}{R} - \rho \Omega^2 R \right) \quad \mu_1 = -\frac{\beta_{11}}{\pi} \quad (91)$$

$$\beta_{22} = \frac{\rho \Omega^2 R}{E_\theta}, \quad \mu_2 = \beta_{22} \left(\frac{\theta - \pi}{\pi} \right)$$

The boundary conditions for this formulation are also homogeneous, as in Eqs. (50) and (51).

This problem can also be solved using an eigensolution, although it is more complicated than the free vibration problem. The system can be represented by the equation:

$$[y]' = [A][y] + [g(\theta)] \quad (92)$$

where

$$[g(\theta)] = [0 \ 0 \ 0 \ \mu_2 \ 0 \ \mu_1]^T \quad (93)$$

Define the matrix $[T]$ as:

$$[T] = \begin{bmatrix} \zeta_{11} & \zeta_{12} & \zeta_{13} & \zeta_{14} & \zeta_{15} & \zeta_{16} \\ \zeta_{21} & \zeta_{22} & \zeta_{23} & \zeta_{24} & \zeta_{25} & \zeta_{26} \\ \zeta_{31} & \zeta_{32} & \zeta_{33} & \zeta_{34} & \zeta_{35} & \zeta_{36} \\ \zeta_{41} & \zeta_{42} & \zeta_{43} & \zeta_{44} & \zeta_{45} & \zeta_{46} \\ \zeta_{51} & \zeta_{52} & \zeta_{53} & \zeta_{54} & \zeta_{55} & \zeta_{56} \\ \zeta_{61} & \zeta_{62} & \zeta_{63} & \zeta_{64} & \zeta_{65} & \zeta_{66} \end{bmatrix} \quad (94)$$

Then let:

$$[y] = [T]^T [x]$$

which implies

$$[x] = [T]^{-T} [y] \quad (95)$$

Then

$$[T]^T [x]' = [A][T]^T [x] + [g(\theta)] \quad (96)$$

Rewriting to isolate $[x]'$

$$[x]' = ([T]^{-T} [A] [T]^T) [x] + [T]^{-T} [g(\theta)] \quad (97)$$

Eq. (97) can be written as:

$$[x]' = [D] [x] + [h(\theta)] \quad (98)$$

where

$$[D] = \begin{bmatrix} \lambda_1 & 0 & 0 & 0 & 0 & 0 \\ 0 & \lambda_2 & 0 & 0 & 0 & 0 \\ 0 & 0 & \lambda_3 & 0 & 0 & 0 \\ 0 & 0 & 0 & \lambda_4 & 0 & 0 \\ 0 & 0 & 0 & 0 & \lambda_5 & 0 \\ 0 & 0 & 0 & 0 & 0 & \lambda_6 \end{bmatrix}$$

and

$$[h(\theta)] = [T]^{-1} [g(\theta)] \quad (99)$$

This transformation uncouples the equations, and so the individual elements of $[x]$ can be written as:

$$x_j(\theta) = e^{\lambda_j \theta} \int_{\theta_0}^{\theta} e^{-\lambda_j \phi} h_j(\phi) d\phi + C_j e^{\lambda_j \theta}, \quad j = 1, 2, 3, 4, 5, 6 \quad (100)$$

For ease of notation, let $[T]^{-T} = [S]$. Writing out $[h(\theta)]$ explicitly

$$[h(\theta)] = [S] \begin{bmatrix} 0 \\ 0 \\ 0 \\ \mu_2 \\ 0 \\ \mu_1 \end{bmatrix} = \begin{bmatrix} (s_{14} \mu_2 + s_{16} \mu_1) \\ (s_{24} \mu_2 + s_{26} \mu_1) \\ (s_{34} \mu_2 + s_{36} \mu_1) \\ (s_{44} \mu_2 + s_{46} \mu_1) \\ (s_{54} \mu_2 + s_{56} \mu_1) \\ (s_{64} \mu_2 + s_{66} \mu_1) \end{bmatrix} \quad (101)$$

where s_{ij} = an element of $[S]$. Eq. (101) can also be written in the form

$$h_j(\theta) = (s_{j4} \mu_2 + s_{j6} \mu_1) \quad (102)$$

where

$$\mu_2 = \beta_{22} \left(\frac{\theta - \pi}{\pi} \right) \quad \text{and} \quad \mu_1 = -\frac{\beta_{11}}{\pi}$$

Next to be determined is the integral

$$\int_{\theta_0}^{\theta} e^{-\lambda_j \phi} h_j(\phi) d\phi = \int_{\theta_0}^{\theta} e^{-\lambda_j \phi} \left[s_{j4} \left\{ \beta_{22} \left(\frac{\theta - \pi}{\pi} \right) \right\} + s_{j6} \left(-\frac{\beta_{11}}{\pi} \right) \right] d\phi \quad (103)$$

Taking this integral and applying the boundary conditions where $\theta_0 = 0$ yields:

$$\begin{aligned} \int_0^{\theta} e^{-\lambda_j \phi} h_j(\phi) d\phi &= s_{j4} \left(\frac{\beta_{22}}{\pi} \right) \left(\frac{1}{\lambda_j} \right)^2 \{ 1 - e^{-\lambda_j \theta} (\lambda_j \theta + 1) \} \\ &+ \left\{ s_{j4} (\beta_{22}) + s_{j6} \left(\frac{\beta_{11}}{\pi} \right) \right\} \left(\frac{1}{\lambda_j} \right) (e^{-\lambda_j \theta} - 1) \end{aligned} \quad (104)$$

This further implies that:

$$\begin{aligned}
 x_j(\theta) = & e^{\lambda_j \theta} \left[s_{j4} \left(\frac{\beta_{22}}{\pi} \right) \left(\frac{1}{\lambda_j} \right)^2 \{1 - e^{-\lambda_j \theta} (\lambda_j \theta + 1)\} \right] \\
 & + e^{\lambda_j \theta} \left[\left\{ s_{j4} (\beta_{22}) + s_{j6} \left(\frac{\beta_{11}}{\pi} \right) \right\} \left(\frac{1}{\lambda_j} \right) (e^{-\lambda_j \theta} - 1) + C_j \right]
 \end{aligned} \tag{105}$$

To determine the unknown constants C_j , the boundary conditions on y at $\theta = 0$ and $\theta = \pi$ are used. They are applied as follows:

$$[y] = [T] [x]$$

$$y_i(\theta) = \sum_{j=1}^6 \zeta_{ij} x_j(\theta) \tag{106}$$

For $\theta = 0$

$$x_j(0) = C_j \tag{107}$$

For $\theta = \pi$

$$\begin{aligned}
 x_j(\pi) = & e^{\lambda_j \pi} \left[s_{j4} \left(\frac{\beta_{22}}{\pi} \right) \left(\frac{1}{\lambda_j} \right)^2 \{1 - e^{-\lambda_j \pi} (\lambda_j \pi + 1)\} \right] \\
 & + e^{\lambda_j \pi} \left[\left\{ s_{j4} (\beta_{22}) + s_{j6} \left(\frac{\beta_{11}}{\pi} \right) \right\} \left(\frac{1}{\lambda_j} \right) + C_j \right]
 \end{aligned} \tag{108}$$

Actually applying the boundary conditions is complicated, so they are written out separately as:

$$\begin{aligned}
y_1(0) = 0 &\rightarrow \sum_{j=1}^6 \zeta_{1j} C_j = 0 \\
y_2(0) = 0 &\rightarrow \sum_{j=1}^6 \zeta_{2j} C_j = 0 \\
y_3(0) = 0 &\rightarrow \sum_{j=1}^6 \zeta_{3j} C_j = 0 \\
y_1(\pi) = 0 &\rightarrow \sum_{j=1}^6 \zeta_{1j} x_j(\pi) = 0 \\
y_2(\pi) = 0 &\rightarrow \sum_{j=1}^6 \zeta_{2j} x_j(\pi) = 0 \\
y_3(\pi) = 0 &\rightarrow \sum_{j=1}^6 \zeta_{3j} x_j(\pi) = 0
\end{aligned} \tag{109}$$

It is necessary to isolate the C_j terms. This is relatively easy for the boundary conditions at $\theta = 0$ but is slightly more complicated in the $\theta = \pi$ terms, so, again, going step by step:

$$\begin{aligned}
\sum_{j=1}^6 \zeta_{ij} x_j(\pi) &= 0 \\
&\rightarrow \sum_{j=1}^6 \zeta_{ij} e^{\lambda_j \pi} \left[s_{j4} \left(\frac{\beta_{22}}{\pi} \right) \left(\frac{1}{\lambda_j} \right)^2 \{1 - e^{-\lambda_j \pi} (\lambda_j \pi + 1)\} \right] \\
&+ \sum_{j=1}^6 \zeta_{ij} e^{\lambda_j \pi} \left[\left\{ s_{j4} (\beta_{22}) + s_{j6} \left(\frac{\beta_{11}}{\pi} \right) \right\} \left(\frac{1}{\lambda_j} \right) (e^{-\lambda_j \pi} - 1) + C_j \right] = 0 \quad i = 1,2,3 \tag{110}
\end{aligned}$$

This implies that:

$$\sum_{j=1}^6 C_j \zeta_{ij} e^{\lambda_j \pi} = - \sum_{j=1}^6 \zeta_{ij} e^{\lambda_j \pi} \left[s_{j4} \left(\frac{\beta_{22}}{\pi} \right) \left(\frac{1}{\lambda_j} \right)^2 \{1 - e^{-\lambda_j \pi} (\lambda_j \pi + 1)\} \right]$$

$$- \sum_{j=1,6}^6 \zeta_{ij} e^{\lambda_j \pi} \left[\left\{ s_{j4} (\beta_{22}) + s_{j6} \left(\frac{\beta_{11}}{\pi} \right) \right\} \left(\frac{1}{\lambda_j} \right) (e^{-\lambda_j \pi} - 1) \right] \quad (111)$$

The complete system which arises from applying the boundary conditions is:

$$\begin{bmatrix} \zeta_{11} & \zeta_{21} & \zeta_{31} & \zeta_{41} & \zeta_{51} & \zeta_{61} \\ \zeta_{12} & \zeta_{22} & \zeta_{32} & \zeta_{42} & \zeta_{52} & \zeta_{62} \\ \zeta_{13} & \zeta_{23} & \zeta_{33} & \zeta_{43} & \zeta_{53} & \zeta_{63} \\ \zeta_{11} e^{\lambda_1 \pi} & \zeta_{21} e^{\lambda_2 \pi} & \zeta_{31} e^{\lambda_3 \pi} & \zeta_{41} e^{\lambda_4 \pi} & \zeta_{51} e^{\lambda_5 \pi} & \zeta_{61} e^{\lambda_6 \pi} \\ \zeta_{12} e^{\lambda_1 \pi} & \zeta_{22} e^{\lambda_2 \pi} & \zeta_{32} e^{\lambda_3 \pi} & \zeta_{42} e^{\lambda_4 \pi} & \zeta_{52} e^{\lambda_5 \pi} & \zeta_{62} e^{\lambda_6 \pi} \\ \zeta_{13} e^{\lambda_1 \pi} & \zeta_{23} e^{\lambda_2 \pi} & \zeta_{33} e^{\lambda_3 \pi} & \zeta_{43} e^{\lambda_4 \pi} & \zeta_{53} e^{\lambda_5 \pi} & \zeta_{63} e^{\lambda_6 \pi} \end{bmatrix} \begin{bmatrix} C_1 \\ C_2 \\ C_3 \\ C_4 \\ C_5 \\ C_6 \end{bmatrix} = - \begin{bmatrix} 0 \\ 0 \\ 0 \\ k_1 \\ k_2 \\ k_3 \end{bmatrix} \quad (112)$$

where

$$k_i = \sum_{j=1}^6 \zeta_{ij} e^{\lambda_j \pi} \left[s_{j4} \left(\frac{\beta_{22}}{\pi} \right) \left(\frac{1}{\lambda_j} \right)^2 \{ 1 - e^{-\lambda_j \pi} (\lambda_j \pi + 1) \} \right] \\ + \sum_{j=1}^6 \zeta_{ij} e^{\lambda_j \pi} \left[\left\{ s_{j4} (\beta_{22}) + s_{j6} \left(\frac{\beta_{11}}{\pi} \right) \right\} \left(\frac{1}{\lambda_j} \right) (e^{-\lambda_j \pi} - 1) \right] \quad i = 1, 2, 3 \quad (113)$$

This system can be written as another $[A][c] = [b]$ matrix equation, and can also be solved by standard means. The coefficient matrix $[A]$ is the same matrix as in the free-vibration section, and the magnitude of the solution vector $[c]$ goes to infinity as the determinant of $[A]$ goes to zero.

This creates the resonance peak, as shown in Fig. (15).

The displacements generated are complex quantities. The magnitude of these numbers is what is plotted on the resonance peak. The

$$\tan^{-1} \left(\frac{\text{IM}(w)}{\text{RE}(w)} \right) = \phi \quad (114)$$

Resonance Peak

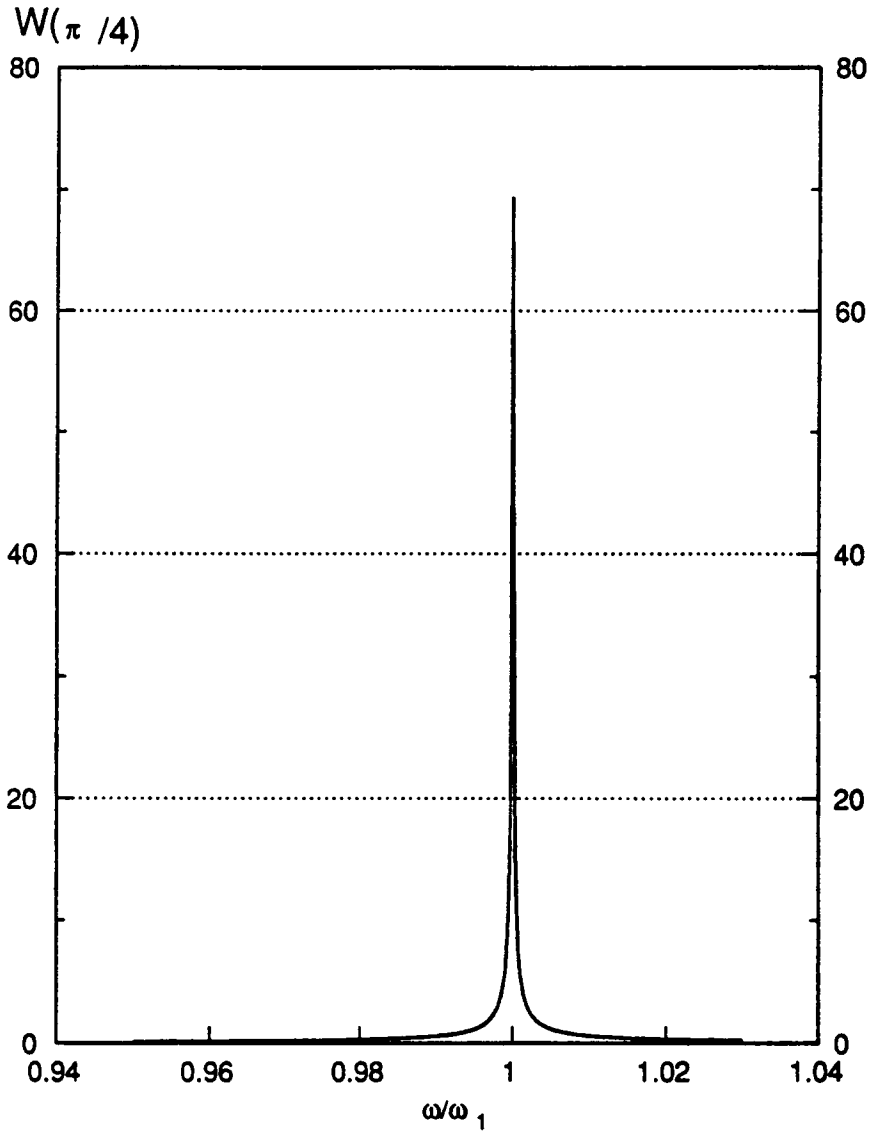


Figure 15. Resonance peak: amplitude of radial vibration at $\theta = \pi/4$ for forcing frequencies around the first natural frequency

is known as the phase angle or phase shift of the response. In this case, there is no damping, which results in a phase angle of $\phi = 0$. The phase shift and damping are discussed in some detail in Chapter 5, special topics, under viscoelasticity.

Fourier Transformations

Any general periodic function, $h(t)$ can be expressed in terms of its Fourier components, which is to say:

$$A(\omega) + i B(\omega) = \int_{-\infty}^{\infty} h(t) e^{i\omega t} dt$$

or, when frequency is in Hertz (cycles per second)

$$A(\omega) + i B(\omega) = \int_{-\infty}^{\infty} h(t) e^{i2\pi f t} dt \quad (115)$$

where $\omega = 2\pi f$ and t is measured in seconds. Given some function $h(t)$, it is possible to create the vectors $A(\omega)$ and $B(\omega)$ such that A and B are the Fourier coefficients of h [10]. However, this can only be done for a finite number of points, and doing so changes the system from a continuous problem to a discretized one. This brings into play the considerations of sampling and aliasing. Define Δ as the time interval between consecutive samples, such that $1/\Delta$ is the number of samples per unit time ; then there exists a special frequency, f_c , called the Nyquist frequency, which is defined: $f_c \equiv 1/2\Delta$. If a given function,

$$H(\omega) = A(\omega) + i B(\omega) = \int_{-\infty}^{\infty} h(t) e^{i2\pi f t} dt = 0 \quad (116)$$

for all frequencies $|f| \geq f_c$, then it can be completely determined by sampling at a time interval Δ .
 If, for some function, $h(t)$

$$|H(\omega)| > 0 \text{ for } |f| > f_c$$

then the power spectral density of the range outside the range $-f_c < f < f_c$ is "folded over" into that range and gives a false representation for $H(\omega)$.

To continue with the analysis, assume N consecutive sampled values

$$h_k = h(t_k), \quad t_k = k\Delta, \quad k = 0, 1, \dots, N-1$$

It is possible to get only N points out for the transformed function, so, they are found for the points

$$f_n = \frac{n}{N\Delta}, \quad n = -\frac{N}{2}, \dots, \frac{N}{2}$$

(assuming N is even)

$$H(f_n) = \int_{-\infty}^{\infty} h(t) e^{i2\pi f_n t} dt$$

Then the integral is approximated by the sum:

$$\sum_{k=0}^{N-1} h_k e^{i2\pi f_n t} \Delta = \Delta \sum_{k=0}^{N-1} h_k e^{i2\pi k_n / N} \tag{117}$$

Let

$$H_n = \sum_{k=0}^{N-1} h_k e^{i2\pi k_n / N}$$

then $H(f_n) \approx \Delta H_n$

Now, rather than having n vary from $-N/2$ to $N/2$, let it go from 0 to $N - 1$. This puts the output in a slightly different form, with $f_c = -f_c$ in the middle of the graph, and 0 at either end. Expressed otherwise

$$0 < f < f_c \quad \sim \quad n = 0 \text{ to } n = \frac{N}{2} - 1$$

$$-f_c < f < 0 \quad \sim \quad n = \frac{N}{2} + 1 \text{ to } n = N - 1$$

$$f = f_c = -f_c \quad \sim \quad n = \frac{N}{2} \tag{118}$$

To complete this solution, it is necessary also to define the inverse Fourier transform:

$$h_k = \frac{1}{N} \sum_{n=0}^{N-1} H_n e^{-i2\pi k_n/N} \tag{119}$$

This permits the response of the system to be computed in the following manner. First, compute the frequency response function, as done earlier, for a wide range of Ω . Then compute the Fourier transform of the forcing function, which involves finding the components of the function in terms of $e^{i\Omega t}$, for as many values of Ω as necessary to yield as accurate a solution as desired. Next, calculate an intermediate value by multiplying the frequency response by the Fourier components of the forcing function. Finally, calculate the inverse Fourier transform of this intermediate value to obtain the response of each point for a time range of 0 to $N\Delta$ seconds.

The frequency response function was computed in the previous section, so all that remains is to choose the forcing functions and compute their Fourier components. To demonstrate the method, three different forcing functions were chosen. To avoid the problem of aliasing, the Fourier transforms were computed by using integrals of continuous functions, rather than transforming an array of discretely sampled points. The functions were

$$F_1(t) = \begin{cases} 1 & 0 \leq t \leq 0.1\text{second} \\ 0 & t > 0.1\text{second} \end{cases} \quad (120)$$

$$F_2(t) = \begin{cases} t & 0 \leq t \leq 0.3\text{second} \\ 1 & t > 0.3\text{second} \end{cases} \quad (121)$$

$$F_3(t) = \sin(t) \quad (122)$$

These functions are shown, along with their Fourier components, in Figs. (16) - (18).

There were only a few necessary changes made in the frequency response function. One was in the output format. Because it is a function of ω^2 , an even function of ω , it was a relatively simple matter to "mirror" the function back to zero. The other change was in the frequency range. The width of the resonance peak is very narrow, as can be seen in Fig. (15). It would be necessary to sample a large number of points, very closely spaced, in order to get an accurate representation of the peak. There would have to be a correspondingly large number of closely spaced points taken on the Fourier transform to yield the same size array to multiply with the frequency response function. This proved to be very costly in terms of computer time, and so a manipulation of the system parameters was performed. The resonance peak is in terms of ω/ω_1 . It is the same no matter what the numerical value for the first frequency happens to be. Because the form of the non-dimensional frequency is $\rho \omega^2/E_\theta$, it was decided to reduce ρ to create an artificially high value of ω_1 . This meant that the sample spacing could be broader in terms of actual units such as Hertz. For example, instead of computing the value of the frequency response function at every 0.001 Hertz, it could be done in 0.01 or even 0.1 Hertz, which lead to a much easier time when computing Fourier transforms back and forth. Fig. (19) is a typical frequency response function for a

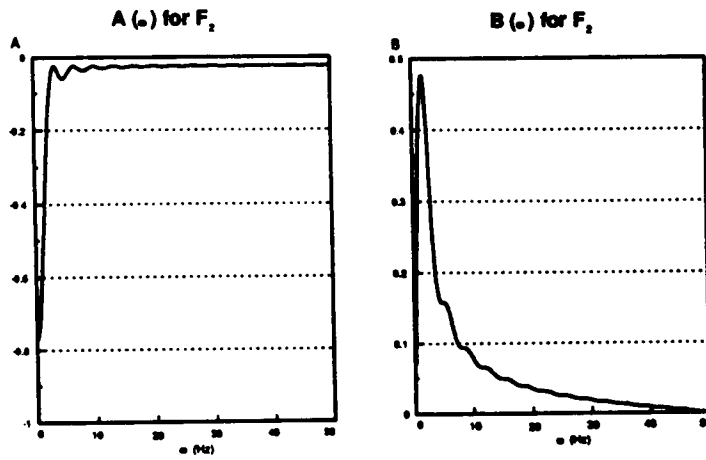
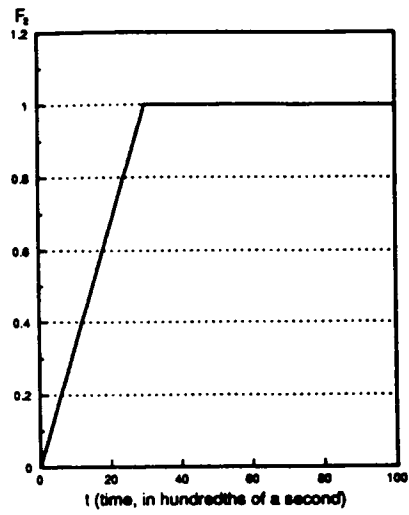


Figure 16. F sub 1 (t): simple step function

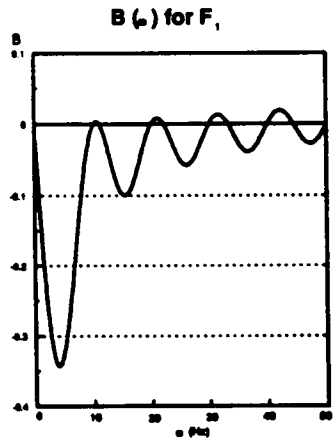
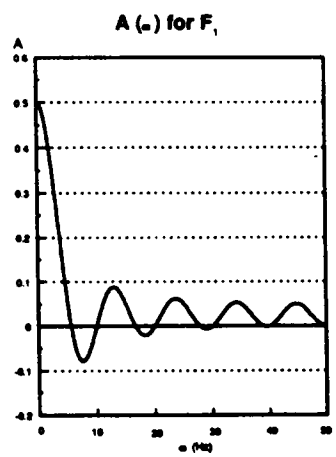
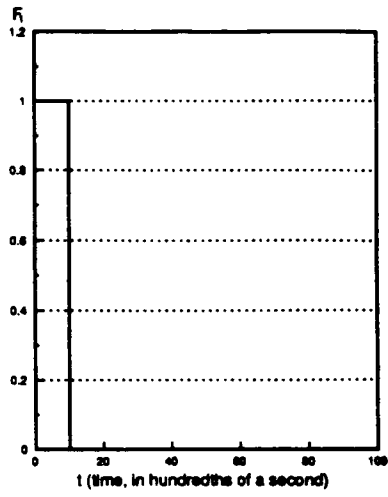


Figure 17. $F_{sub 2}(t)$: ramp up to straight line

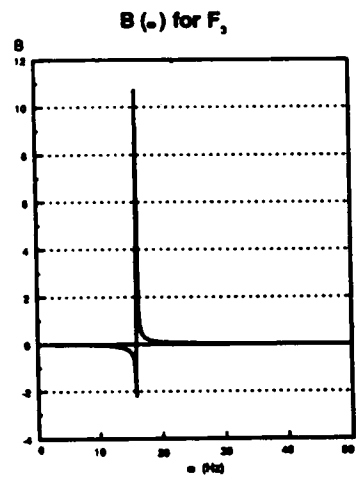
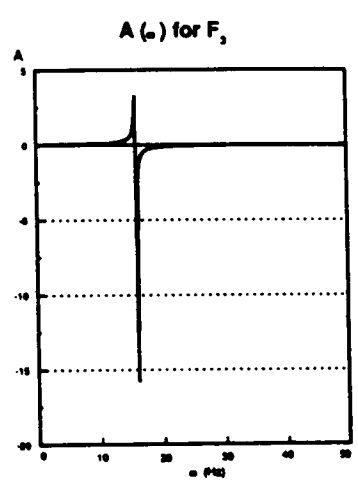
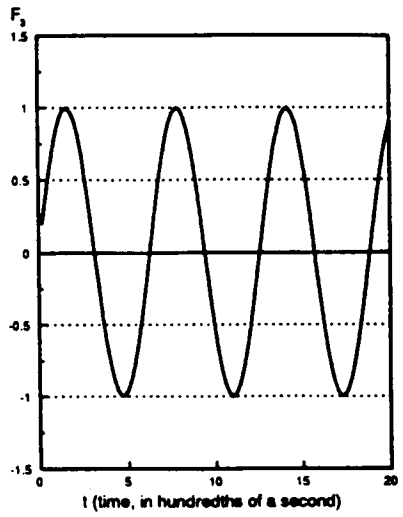


Figure 18. $F_{sub 3}(t)$: sine wave

Frequency Response Function

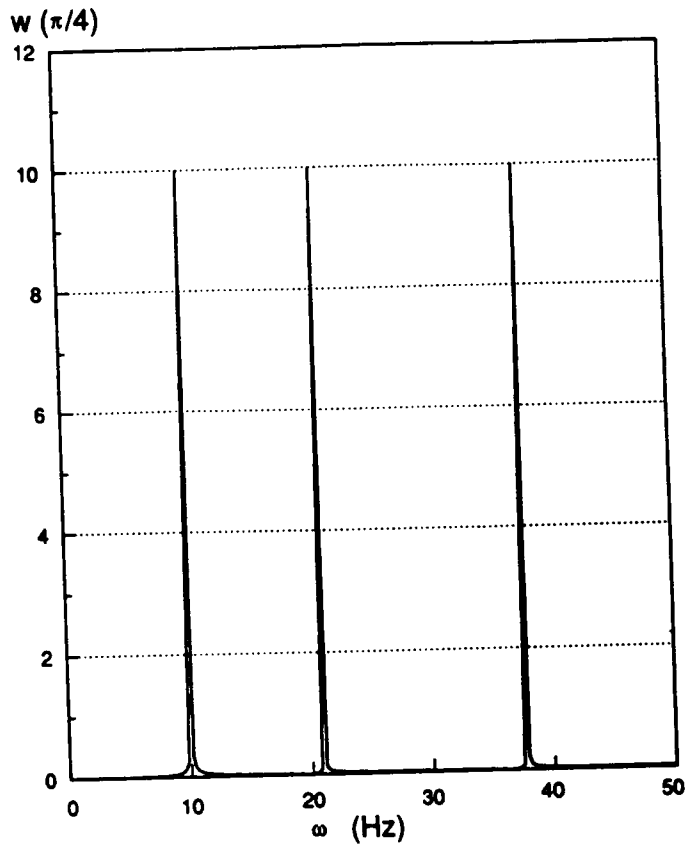


Figure 19. Frequency response function: frequency response function in the format necessary for the forced response

single point on the graph, for the range on ω necessary for the Fourier transform. The w , radial response at the point $\theta = \pi/4$ to the excitations F_1 , F_2 , and F_3 are shown in Fig. (20).

This concludes the model for the arch and completes the solution of the vibration problem.

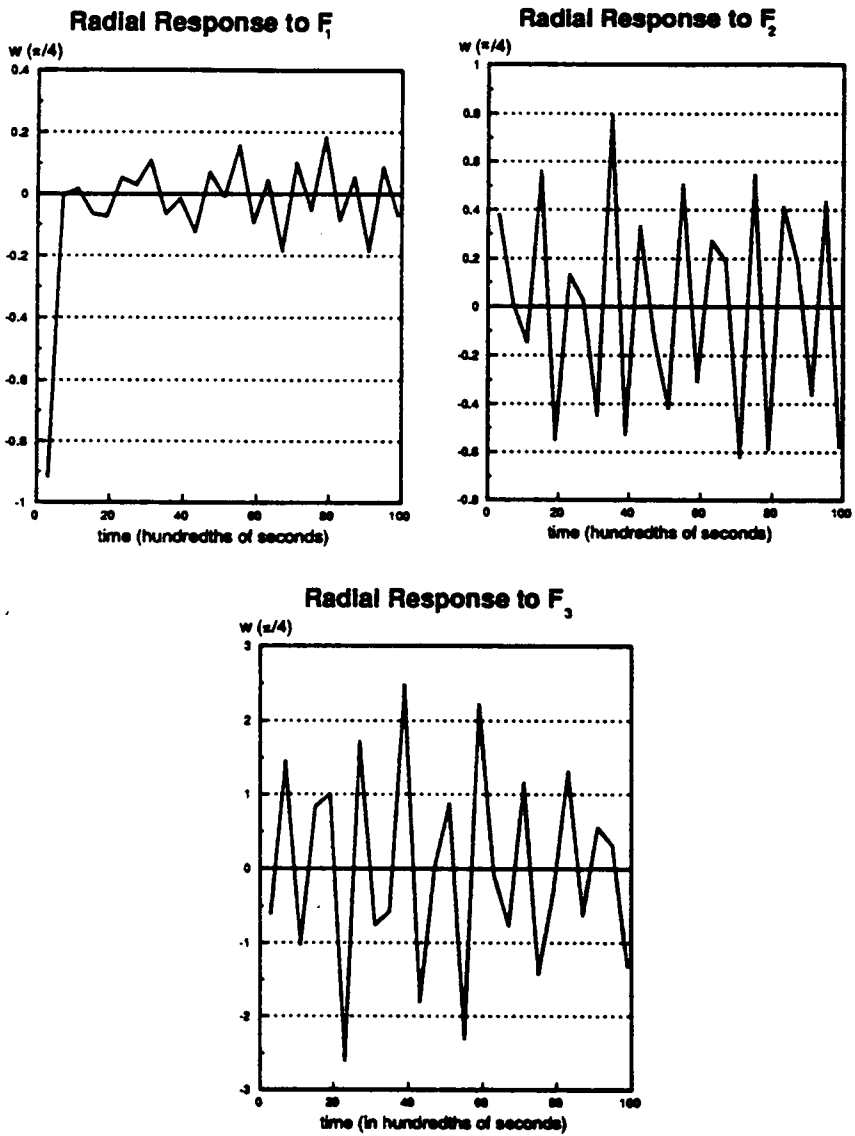


Figure 20. Radial response: radial response of point theta = pi/4 subject to forcing functions, F1, F2, and F3

Chapter 5

SPECIAL TOPICS

Viscoelasticity

Damping, or viscoelasticity, was introduced to the model by means of a complex modulus. The matrix is far more likely to contribute to the damping of the system, so the matrix modulus is expressed as a complex quantity:

$$E_1 = |E_1|(1 + \zeta i)$$

where $|E_1|$ is the magnitude of the elastic modulus, and ζ is known as the damping factor, which is a measure of the material viscoelasticity. This type of damping is referred to as structural, as opposed to viscous damping. Mathematically, this means that the coefficient of every term in the equations of motion, Eqs. (47) and (48), is complex, whereas in viscous damping only the velocity and other odd time derivatives of position have coefficients that contribute to the system damping.

According to Meirovitch [11], structural damping can have several effects. One of these is known as the hysteresis loop. The effect of structural damping on the resonance peak is one of the most noticeable differences with viscous damping. The peak of the resonance graph shifts slightly with increasing ζ , and occurs at a damped natural frequency, defined as:

$$\omega_d^2 = \sqrt{\omega_n^2 - \zeta^2}$$

With structural damping there is no such shift in the peak as long as the excitation is sinusoidal in nature, which is exactly the case when $F = e^{i\omega t}$. The damping has very little effect on amplitude, except right at resonance, as in Fig. (21): however, there is a phase shift, as in the viscously damped system. This effect can be seen in Fig. (22). The shift goes from about π , or 180° out of phase with the excitation, to about 0° , or in phase with the excitation, as the arch goes from one mode shape to the next.

The other effects of damping can be seen in the response of a system with damping to the same forcing functions F_1 , F_2 , and F_3 that were used in Chapter 4. Although not quite so dramatic a difference as in the phase shift, the effects of damping can be seen in Figs. (23) - (25), where the absolute value of the response is shown for both the damped and undamped systems. The effect of damping on amplitude is noticeable, especially at the low end. The phase shift is not noticeable at this degree of damping, as might be expected from examining the resonance peak, Fig. (21), because there is very little reduction in the height of the peak for $\zeta = 0.01$.

Determination of Modulus

The motivation behind this model of an arch was to interpret and possibly to correlate with data from the Dynamic Mechanical Analyzer. With this in mind, a graph of ω_1 vs E_θ was created for several values of E_2 . Several values of E_2 were used because the statically determined value was the one used as data for the model, but the dynamic value could be significantly different. A range

Damped Resonance Peak

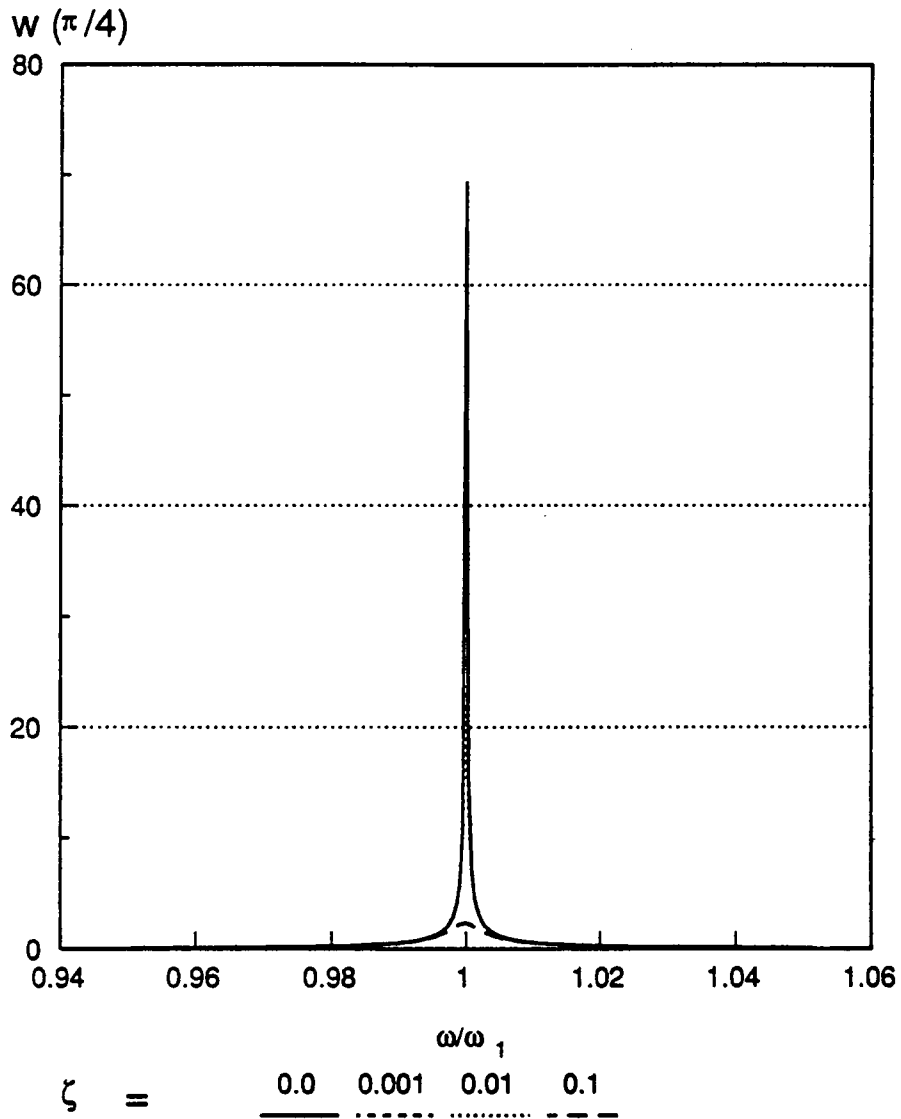


Figure 21. Damped Resonance Peak: radial displacement at $\theta = \pi/4$ around the first natural frequency

Phase Shift

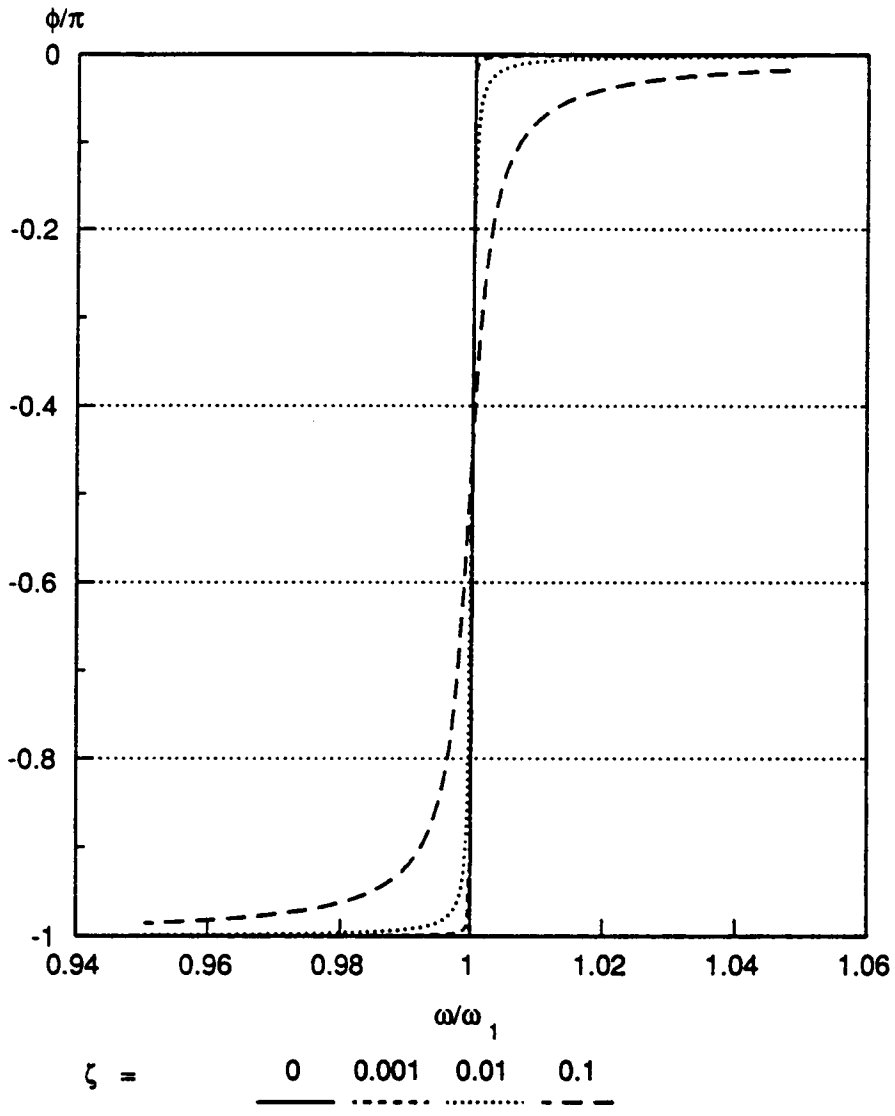


Figure 22. Phase shift: phase shift for radial displacement at $\theta = \pi/4$ around the first natural frequency

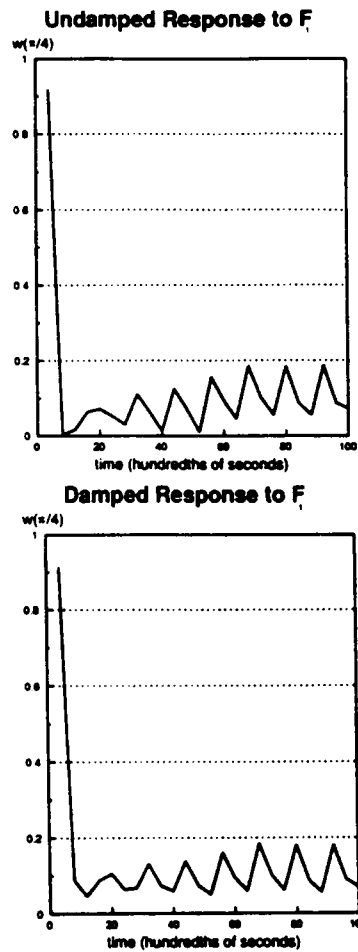


Figure 23. Damped response for F_1 : radial response at $\theta = \pi/4$ for damped and undamped cases

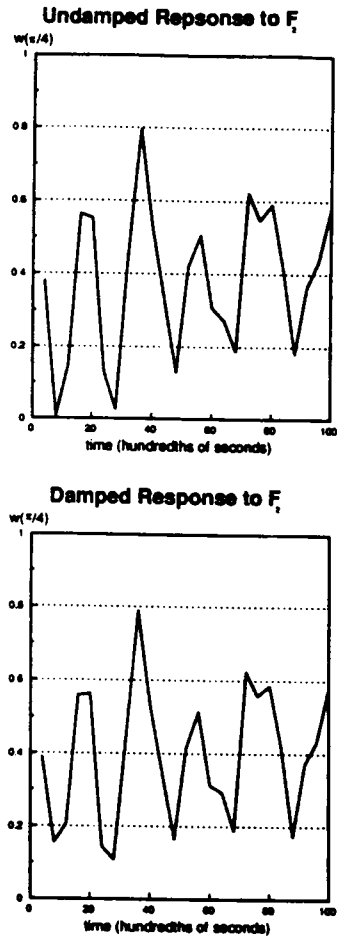


Figure 24. Damped response for F_2 : radial response at $\theta = \pi/4$ for damped and undamped cases

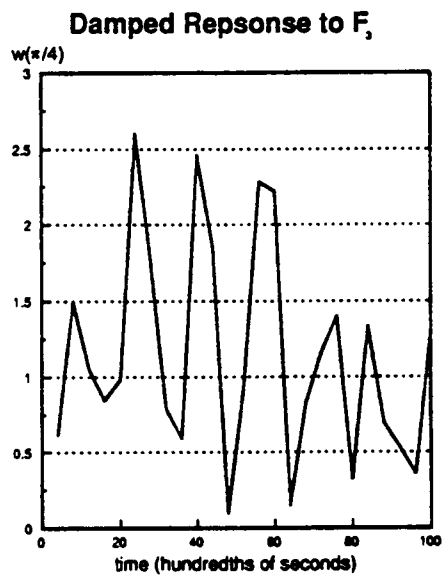
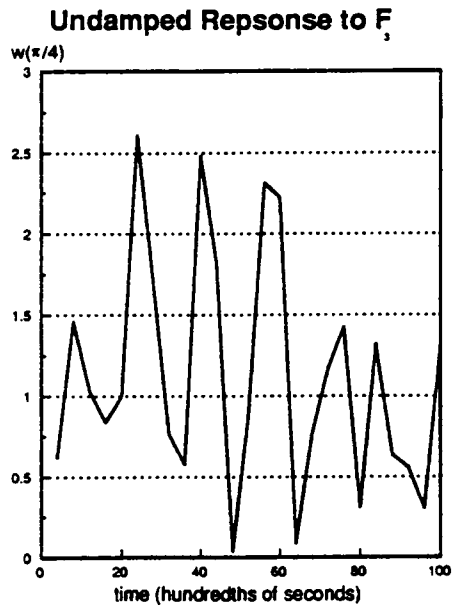


Figure 25. Damped response for F3: radial response at $\theta = \pi/4$ for damped and undamped cases

of values around the static one were used to generate this graph so that once a dynamic value for E_x is determined, the graph could be used to indicate a value for E_θ .

As expected, the value of ω_1 increased linearly with E_θ , because in its dimensionless form $\omega^2 = \rho \bar{\omega}^2 / E_\theta$. The differences between the computed value of ω for different values of E_x were more pronounced at the higher values of E_θ .

Then, using Fig. (26) as a guide, the data from the DMA was used as input to a program which determined the modulus of the arch, given the first natural frequency. The data was in the form of Fig. (27), which has both ω_1 and E_θ versus temperature. The idea was to take the value for ω_1 and see what the predicted value for E_θ was, and then compare that to the value computed by the DMA. The results of this comparison can be seen in Fig. (28). The match between model and experimental data is reasonable except at the extremes of temperature. The model does not predict the same value for E_θ as the DMA computed at these points, but this is only to be expected, because the model did not account for any effects of temperature, other than the change in natural frequency, and used data for material constants other than E_θ that was acquired at room temperature static tests. In general, it would seem that the value predicted by the model confirms the value computed by the DMA, with some deviation at the temperature extremes, and, although it is less than an exact match with DMA, it is a reasonable model of the system.

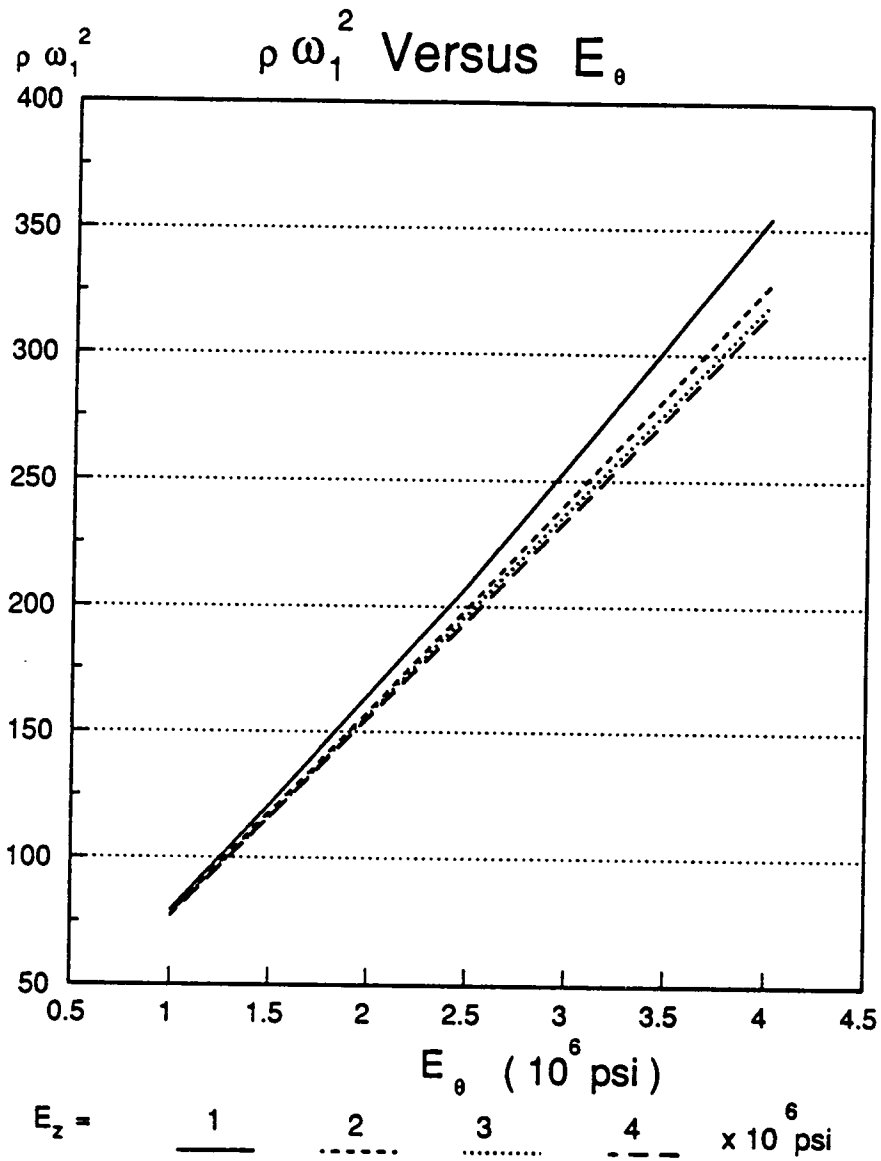


Figure 26. ω_1 vs E_θ : first natural frequency as a function of E_θ , for several values of E_z

Sample : RING COMPOSITE
Size : 84.28 x 8.30 x 1.28 mm
Method : COMPOSITE
Comment :

DMA

File : E:RING.01
Operator: TOM
Run Date: 04/04/88 16:18

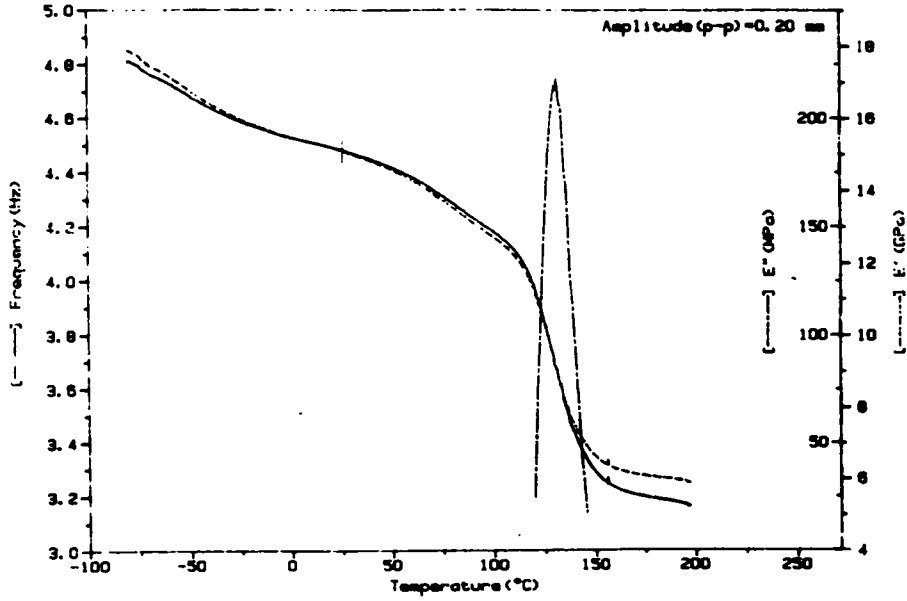


Figure 27. Data from a DMA test

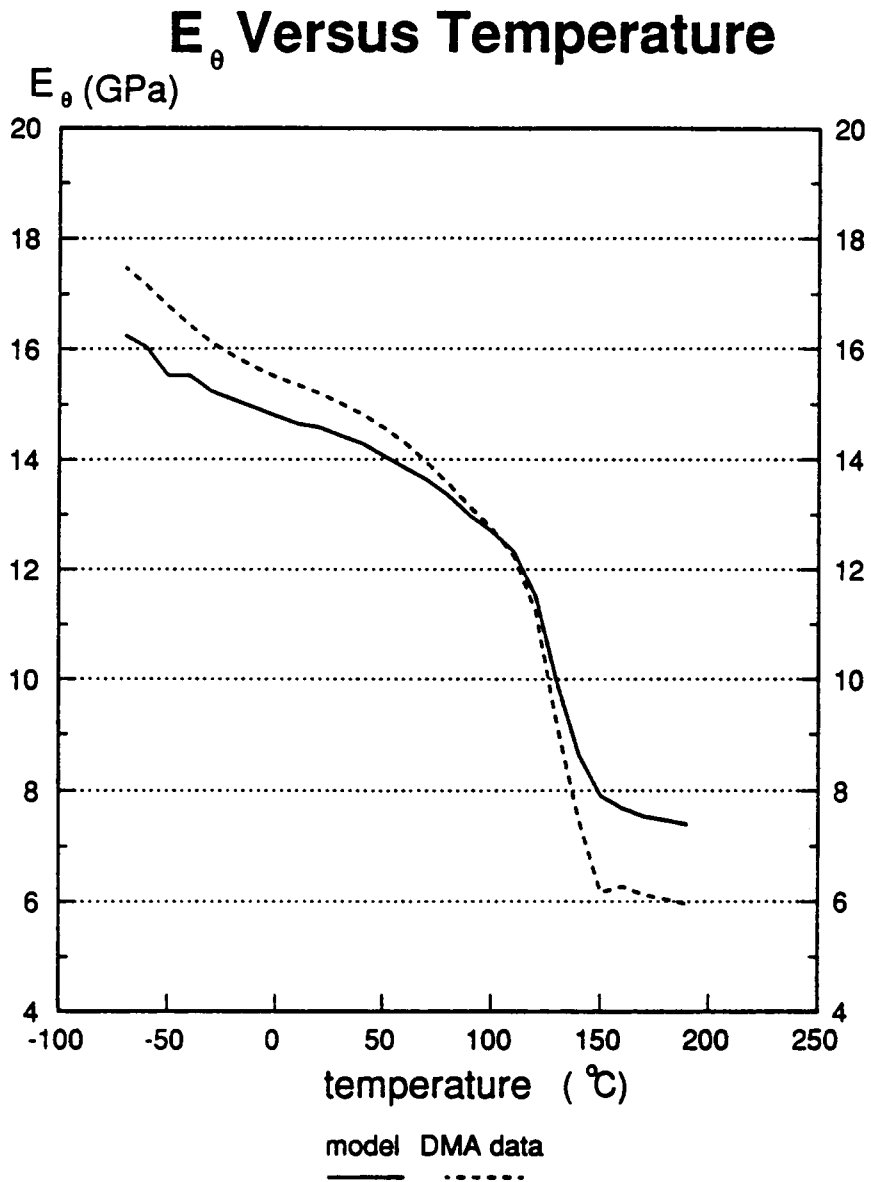


Figure 28. E_{θ} vs temperature: values for E_{θ} as predicted by the model, and as computed by the DMA

Conclusions

The principles employed here imply that it is possible to incorporate into a model of an arch anything that is being done for shells, such as non-linear effects, or the inclusion of stiffeners, by simply neglecting the variation of variables across the width of the shell, thereby making it an arch. The resulting system of equations can then be solved by whatever means are appropriate to the particular problem.

Here, a model for the in-plane vibrations of an arch was developed using standard models for a shell. It can be used to predict the right range of natural frequency as compared to existing models, and to experimental data. The mode shapes are also in agreement with the existing models, and with those observed experimentally. This is a workable solution; it is possible to obtain many natural frequencies before encountering problems with numerical stability. The solution is easy to modify. It is only necessary to add terms to the coefficient matrix, for example, to account for such effects as shear deformation or rotatory inertia. The solution technique remains the same, even when considering a more complicated material system that recouples the equations of motion.

The technique can handle a general forcing function, as in this case with the one end excitation. It can also include other types of loading, such as pressure loading. These terms were dropped in derivation, but could certainly be included with little additional effort. The model incorporates structural damping, yielding the expected resonance peak and phase shift. Finally, the

results agree well with the experimental data that the model was designed to check. Some topics for future consideration include a study of random loading for fatigue data, or a parametric study for design purposes.

Bibliography

1. Fuchs, Hannes Personal communication, Feb. (1989).
2. Whitney, J. M., *Structural Analysis of Laminated Anisotropic Plates*, Technomic Publishing Co., (1987).
3. Flugge, W., *Stresses in Shells*, Springer-Verlag, (1973).
4. Jones, R., *Mechanics of Composite Materials*, Scripta Book Co. Washington, DC, (1975).
5. Archer, R. R., "Small Vibrations of Thin Incomplete Circular Rings," *International Journal of Mechanical Sciences*, Vol. 1, (1960): 45-56.
6. Meile, A., "Method of Particular Solutions for Linear Two-Point Boundary Value Problems," *Journal of Optimization Theory and Applications*, Vol. 2, No. 4, (1968): 260-273.
7. Franklin, J., *Matrix Theory*, Prentice Hall, Englewood Cliffs, NJ, (1968).
8. Boyce and DiPrima *Elementary Differential Equations and Boundary Value Problems, Third edition* John Wiley & Sons, NY, (1977): 265-336.
9. Collins, J. S., and Johnson, E. R., "Free Vibrations of Semi Circular Graphite Epoxy Rings with Open Sections," *Proceedings of the Sixth Annual Review*, of the Center for Composite Materials and Structures, at Virginia Polytechnic Institute and State University, 9-11 April, (1989): P1 - P13.
10. Press, W. H., Flannery, B. P., Teukolsky, S. A., and Vetterling, W. T., *Numerical Recipes*, Cambridge University Press, (1986): 381-453.
11. Meirovitch, L., *Elements of Vibration Analysis, second edition*, McGraw-Hill Inc. (1976, 1985).

Additional Reading

Included here is a fairly comprehensive list of sources available on the vibrations of arches. Most of the references in this list were not used directly in the model explored in this study, but were a useful background in developing it. Anyone interested in the vibrations of arches should be aware of the work that has already been done in the field, and these sources should provide a convenient starting point for further research.

- Archer, R. R., "Small Vibrations of Thin Incomplete Circular Rings," *International Journal of Mechanical Sciences*, Vol. 1, 1960, pp. 45-56.
- Bellow, D.G. and Semeniuk, A., "Symmetrical and Unsymmetrical Forced Excitation of Thin Circular Arches," *International Journal of Mechanical Sciences*, Vol. 14., 1972, pp. 185-195.
- Bhattacharya, A. P., "Large-Amplitude Vibrations of Imperfect Cross-Ply Laminated Cylindrical Shell Panels with Elastically Restrained Edges and Restrained Edges and Resting on Elastic Foundation," *Fibre Science and Technology*, Vol. 21, 1984, pp. 205-221.
- Brown, F. H., "Lateral Vibration of Ring-Shaped Frames," *Journal of the Franklin Institute*, Vol. 218, July 1934, pp. 41-48.
- Brunelle, E. J., "The Statics and Dynamics of a Transversely Isotropic Timoshenko Beam," *Journal of Composite Materials*, Vol. 4, July, 1970, pp.404-416.

- Brunelle, E. J., "Elastic Instability for Transversely Isotropic Timoshenko Beams," *AIAA Journal*, Vol.8, No.12, Dec. 1970, pp.2271-2273.
- Collins, J. S., and Johnson, E. R., "Free Vibrations of Semi Circular Graphite Epoxy Rings with Open Sections," *Proceedings of the Sixth Annual Review, Center for Composite Materials and Structures (CCMS) Virginia Polytechnic Institute and State University* Apr.9-11, 1989, pp.P1 - P13.
- Cortinez, V.H., "Numerical Experiments on Vibrating Cantilever Arches of Varying Cross-section," *Journal of Sound and Vibration*, Vol. 110, Oct 1986, pp. 356-358.
- Cortinez, V.H., "In Plane Vibration of a Clamped Circular Arch System," *Journal of Sound and Vibration*, Vol. 112, No.2 Jan 1987, pp. 379-383.
- Den Hartog, J. P., "The Lowest Natural Frequency of Circular Arcs," *Philosophical Magazine*, Ser. 7, Vol. 5, 1928, pp. 400-408.
- Du, I. and Hui, D. "Frequency-Load Interaction of Imperfect Angle-Ply Cylindrical Panels under Compression and Pressure," *AIAA Journal*, Vol. 25, No. 3, March, 1987, pp. 484-491.
- Ercoli, L., Laura, P. A. A., Filipich, C. P., "Analytical and Experimental Investigation on Vibrating Arches Clamped at One End and Carrying a Concentrated Mass at the Other," *Journal of Sound and Vibration*, Vol. 111 No.2, Dec 1986, pp. 349-351.
- Irie T., Yamada, G., Tanaka, K., "Natural Frequencies of Out of Plane Vibrations of Circular Arcs," *Journal of Applied Mechanics*, Vol. 49, Dec 1982, pp. 910-913.
- Irie T., Yamada, G., Tanaka, K., "Natural Frequency of In Plane Vibration of Arcs," *Journal of Applied Mechanics*, Vol. 50, No.2, Jun 1983, pp. 449-452.
- Issa, M.S., Wang, T.M., and Hsiao, B.T., "Extensional Vibrations of Continuous Circular Curved Beams with Rotary Inertia and Shear Deformation, I Free Vibration," *Journal of Sound and Vibration*, Vol. 114, No. 2, 1987, pp. 297-308.
- Morley, L.S.D., "The Flexural Vibrations of a Cut Thin Ring," *Quarterly Journal of Mechanics and Applied Math*, Vol. 11, No.4, 1958, pp. 491-497.

- Nagaya, K., and Hirano, Y., "In Plane Vibration of a Viscoelastic Circular Rod With Shear Correction Factors and Rotary Inertia," *Bulletin of the JSME*, Vol.20, No. 143, May 1977, pp. 539-547.
- Nagaya, K., and Niiyama, H., "Stress Analysis of a Viscoelastic Solid of Arbitrary Shape Having a Circular Cavity and Subject to Internal Vibration Pressures," *Journal of Sound and Vibration*, Vol. 114, No. 2, 1987, pp. 219-232.
- Pilipchuk, "On Essentially Non-Linear Dynamics of Arches and Rings," *Journal of Applied Math and Mechanics*, Vol. 46, No.3, Jun 1983, pp. 360-364.
- Plaut, R.H., "Oscillations and Instability of a Shallow Arch Under Two-Frequency Excitation," *Journal of Sound and Vibration*, vol. 102, No.2, Sept 1985, pp. 189-201.
- Raithel, A. and Franciosi, C., "Dynamic Analysis of Arches of Varying Cross-section Using a Lagrangian Approach," *Journal of Sound and Vibration*, Vol. 110, No.4, Apr 1984, pp. 847-858.
- Reissner, E., "Note on the Problem of Vibrations of Slightly Curved Bars," *Journal of Applied Mechanics*, June, 1954, pp. 195-196.
- Rossettos, J. N., and Squires, D. C., "Modes and Frequencies of Transversely Isotropic Slightly Curved Timoshenko Beams," *Journal of Applied Mechanics*, Dec. 1973, pp. 1029-1033.
- Rossettos, J. N., "Vibration of Slightly Curved Beams of Transversely Isotropic Composite Materials," *AIAA Journal*, Vol. 9, No. 11, Nov. 1971, pp.2273-2275.
- Sato, K., "Free Flexural Vibrations of an Elliptical Ring in its Plane," *Journal of the Acoustical Society of America*, Vol. 57, Jan 1975, pp. 113-115.
- Teoh, L. S., and Huang, C. C., "The Vibration of Beams of Fibre Reinforced Material," *Journal of Sound and Vibration*, Vol. 51, No.4, 1977, pp.467-473.
- Volterra and Morell, J.D., "Lowest Natural Frequency of Elastic Arc for Vibrations Outside the Plane of Initial Curvature," *Journal of Applied Mechanics*, Vol. 28, 1961, pp. 624-627.
- Volterra, E. Morell, J.D., "A Note on the Lowest Natural Frequency of Elastic Arches," *Journal of Applied Mechanics*, Vol. 27, Dec 1960, pp. 744-746.

- Wang, T.M., "Lowest Natural Frequency of Clamped Parabolic Arcs," *Journal of Engineering Mechanics*, Vol. 98, 1972, pp. 407-411.
- Wang, T.M., and Lee, J.N., "Forced Vibrations of Continuous Circular Arch Frames," *Journal of Sound and Vibration*, Vol. 32, 1974, pp. 159-173.
- Wang, T.M., and Guilbert, M.P., "Effects of Rotary Inertia and Shear on Natural Frequencies of Continuous Circular Curved Beams," *International Journal of Solids and Structures*, Vol. 17, 1981, pp. 281-289.
- Wang, T.M., and Issa, M.S., "Extensional Vibrations of Continuous Curved Beams with Rotary Inertia and Shear Deformation, II Forced Vibrations," *Journal of Sound and Vibration*, Vol. 114, No. 2, 1987, pp. 309-323.
- Wasserman, Y., "The Influence of the Behavior of the Load on the Frequency and Critical Loads of Arches with Flexibly Supported Ends," *Journal of Sound and Vibration*, Vol 54, No.4, 1977, pp. 515-526.
- Wasserman, Y., "Spatial Symmetrical Vibration of Circular Arches with Flexibly Supported Ends," *Journal of Sound and Vibration*, Vol. 59, No.2, Jul 1978, pp. 181-194.
- Wasserman, Y., "Spatial Antisymmetrical Vibrations and Stability of Circular Arches with Flexibly Supported Ends," *Israel Journal of Technology*, Vol. 16, Nos.5-6, 1978, pp. 224-233.
- Wolf, J.A., "Natural Frequencies of Circular Arcs," *Journal of Engineering Mechanics*, Vol. 97, 1971, pp. 2337-2350.

Appendix A

Derivation of [Q]

From the classical theory of elasticity, the stress-strain relations for an orthotropic material can be written:

$$\begin{bmatrix} \sigma_x \\ \sigma_\theta \\ \sigma_r \\ \sigma_{r\theta} \\ \sigma_{rx} \\ \sigma_{x\theta} \end{bmatrix} = \begin{bmatrix} C_{11} & C_{12} & C_{13} & 0 & 0 & 0 \\ C_{21} & C_{22} & C_{23} & 0 & 0 & 0 \\ C_{31} & C_{32} & C_{33} & 0 & 0 & 0 \\ 0 & 0 & 0 & C_{44} & 0 & 0 \\ 0 & 0 & 0 & 0 & C_{55} & 0 \\ 0 & 0 & 0 & 0 & 0 & C_{66} \end{bmatrix} \begin{bmatrix} \varepsilon_x \\ \varepsilon_\theta \\ \varepsilon_r \\ \varepsilon_{r\theta} \\ \varepsilon_{rx} \\ \varepsilon_{x\theta} \end{bmatrix} \quad (A1)$$

For ease of notation, let

$$1 = x, \quad 2 = \theta, \quad \text{and} \quad 3 = r$$

From Jones, [10], the C_{ij} are defined in terms of the standard engineering material constants:

$$\begin{aligned}
C_{11} &= \frac{1 - \nu_{23} \nu_{32}}{E_2 E_3 \Delta}, & C_{12} &= \frac{\nu_{12} + \nu_{32} \nu_{13}}{E_1 E_3 \Delta}, & C_{13} &= \frac{\nu_{13} + \nu_{12} \nu_{23}}{E_1 E_2 \Delta}, \\
C_{22} &= \frac{1 - \nu_{13} \nu_{31}}{E_1 E_3 \Delta}, & C_{23} &= \frac{\nu_{32} + \nu_{12} \nu_{31}}{E_1 E_3 \Delta}, & C_{33} &= \frac{1 - \nu_{12} \nu_{21}}{E_1 E_2 \Delta} \\
C_{44} &= G_{23}, & C_{55} &= G_{31}, & C_{66} &= G_{12}, \\
\Delta &= \frac{1 - \nu_{12} \nu_{21} - \nu_{23} \nu_{32} - \nu_{31} \nu_{13} - 2 \nu_{21} \nu_{32} \nu_{13}}{E_1 E_2 E_3}
\end{aligned} \tag{A2}$$

The material symmetries also imply that

$$\frac{\nu_{ij}}{E_i} = \frac{\nu_{ji}}{E_j} \quad ij = 1,2,3 \tag{A3}$$

Assuming plane stress be setting:

$$\sigma_r = 0, \quad \sigma_{\theta r} = 0, \quad \sigma_{xr} = 0 \tag{A4}$$

the stress-strain relations can be written as

$$\begin{bmatrix} \sigma_x \\ \sigma_\theta \\ \sigma_{x\theta} \end{bmatrix} = \begin{bmatrix} Q_{11} & Q_{12} & 0 \\ Q_{12} & Q_{22} & 0 \\ 0 & 0 & Q_{66} \end{bmatrix} \begin{bmatrix} \varepsilon_x \\ \varepsilon_\theta \\ \varepsilon_{x\theta} \end{bmatrix} \tag{A5}$$

where

$$\begin{aligned}
Q_{11} &= \frac{E_1}{1 - \nu_{12} \nu_{21}}, & Q_{22} &= \frac{E_2}{1 - \nu_{12} \nu_{21}}, \\
Q_{12} &= \frac{\nu_{12} E_2}{1 - \nu_{12} \nu_{21}}, & Q_{66} &= G_{12}
\end{aligned} \tag{A9}$$

This is the relationship employed in the preceding chapters to develop the equations of motion.

Appendix B

Program for Determination of Modulus

```
IMPLICIT REAL *8(A-H,O-Z)
```

```
COMPLEX *16 EVAL(6),EVEC(6,6),CMAT(6,6),DET,MULT,SUM,
```

```
%A(3,3),D(3,3),ALPHA(2,2),BETA(2,2),E1
```

```
REAL *8 NU23,NU13,NU12,DETR(1000),OMEGA2A(1000),TEMP(100)
```

```
C*****
```

```
C EDET COMPUTES THE MODULUS OF A SYSTEM GIVEN ITS
```

```
C NATURAL FREQUENCY
```

```
C USING NUMERICAL TECHNIQUES AND REDUCTION OF ORDER
```

```
C IT IS THE ORTHOTROPIC CASE
```

```
C IT CAN INCLUDE DAMPING
```

```
C*****
```

```
C INPUT: MATERIAL CONSTANTS
```

```
C OUTPUT: NATURAL FREQUENCY (NONDIMENSIONAL)
```

```
C*****
```

```
100 FORMAT(2X,F25.16,10X,F25.16)
```

1001 FORMAT(2X,F14.9,5X,F14.9,10X,F14.9)

140 FORMAT(2X,F25.16)

201 FORMAT(2X,/))

1000 FORMAT(2X,F16.8,10X,E16.8,10X,E16.8)

111 FORMAT(//)

PI = DARCOS(-1.D0)

MULT = (0.D0,-1.D0)

C*****

C STEP ONE: INPUT OR CREATE RANGE OF MATERIAL CONSTANTS

C*****

C SET GEOMETRIC AND MATERIAL CONSTANTS

C NOTE: 1 = X- DIRECTION

C NOTE: 2 = THETA -DIRECTION

C NOTE: 3 = RADIAL -DIRECTION

C*****

E1 = 1.80D6*DCMPLX(1.D0,ZETA)

E3 = E1

E1R = E1

G12 = .5D6

H = 6.811D-2

ARC = 2.50984D-1

RADIUS = 1.70177D0

NU23 = .186D0

NU13 = .0492D0

NU12 = .186D0

RHO = 0.2D0

ZETA = 0.00D0

C*****

C READ THE VALUE FOR OMEGA2 (RADIANS/SECOND**2) AND SET
C OMEGA2A (THE OUTPUT VALUE OF OMEGA)

C*****

DO 700 IW2 = 1,27
READ(4,100) TEMP(IW2),OMEGA2A(IW2)
SAVE = 1.D0
ESAVE = 1.D0
OMEGA = OMEGA2A(IW2)*PI*2.D0
OMEGA2 = OMEGA*OMEGA

C*****

C SET THE VALUE OF E2 FOR ITERATION

C*****

DO 500 IE = 1,200
E2 = 7.D5 + (IE-1)*1.D4

C*****

C STEP TWO: CREATE THE COEFFICIENTS USED IN THE EVP SECTION
C OF THE SOLUTION

C*****

CALL COEFFA(E1,E2,NU12,G12,A,D,H)
CALL COEFF1(ALPHA,BETA,OMEGA2,RADIUS,A,D,E2,RHO)

C*****

C STEP THREE: CALL THE SUBROUTINE TO FIND THE EV

C*****

CALL ANUM(ALPHA,BETA,EVAL,EVEC)

C*****

C STEP FOUR: CREATE THE COEFFICIENT MATRIX TO EVALUATE THE
C CONSTANTS USING THE BOUNDARY CONDITIONS

C*****

```

CALL AMAT(EVAL,EVEC,PI,CMAT)
C*****
C STEP FIVE: TAKE THE DETERMINANT OF THE MATRIX CMAT
C*****
CALL CINV(CMAT,DET)
DETR(IW2) = CDABS(DET)
C*****
C FIND AND SAVE THE SMALLEST DETERMINANT, AND THE VALUE OF THE
C MODULUS AT THAT POINT
C*****
IF(SAVE.GT.DETR(IW2)) THEN
SAVE = DETR(IW2)
ESAVE = E2
END IF
C*****
500 CONTINUE
C*****
C OUTPUT OF RESULTS
C*****
ESAVE = ESAVE/1.D6
WRITE(7,1001) TEMP(IW2),ESAVE,SAVE
700 CONTINUE
C*****
STOP
END
C*****
SUBROUTINE COEFFA(E1,E2,NU12,G12,A,D,H)
C*****

```

```

    IMPLICIT REAL *8(A-H,O-Z)
    REAL *8 NU23,NU13,NU12
    COMPLEX*16 Q(3,3),A(3,3),D(3,3),E1,FACT
    DO 10 I= 1,3
    DO 10 J= 1,3
10  Q(I,J)= 0.D0
    FACT= E1-NU12*NU12*E2
    Q(1,1)= E1*E1/FACT
    Q(1,2)= NU12*E1*E2/FACT
    Q(2,2)= E1*E2/FACT
    Q(3,3)= G12
    DO 15 I= 1,3
    DO 15 J= 1,3
15  Q(J,I)= Q(I,J)
C*****
    DO 20 I= 1,3
    DO 20 J= 1,3
    A(I,J)= Q(I,J)*H
20  D(I,J)= A(I,J)*H*H/12.D0
    RETURN
    END
C*****
    SUBROUTINE COEFF1(ALPHA,BETA,OMEGA2,R,A,D,E2,RHO)
C*****
    IMPLICIT REAL *8 (A-H,O-Z)
    COMPLEX *16 ALPHA(2,2),BETA(2,2),A(3,3),D(3,3)
    DO 20 I= 1,2
    DO 20 J= 1,3

```

```

ALPHA(I,J) = 0.D0
20 BETA(I,J) = 0.D0
ALPHA(1,1) = D(2,2)/(E2*R*R*R)
ALPHA(1,2) = A(2,2)/(R*E2)-(OMEGA2*RHO*R/E2)
ALPHA(2,1) = A(2,2)/(E2*R)
BETA(1,1) = ALPHA(2,1)
BETA(2,1) = ALPHA(2,1)
BETA(2,2) = OMEGA2*RHO*R/E2
RETURN
END

```

```

C*****

```

```

SUBROUTINE ANUM(ALPHA,BETA,EVAL,EVEC)

```

```

C*****

```

```

IMPLICIT REAL*8 (A-H,O-Z)

```

```

COMPLEX *16 ALPHA(2,2),BETA(2,2),A(6,6)

```

```

%,EVAL(6),EVEC(6,6),LENGTH(6),DET

```

```

100 FORMAT(2X,E25.16)

```

```

111 FORMAT(//)

```

```

DO 10 I = 1,6

```

```

DO 10 J = 1,6

```

```

10 A(I,J) = 0.D0

```

```

A(1,3) = 1.D0

```

```

A(2,4) = 1.D0

```

```

A(3,5) = 1.D0

```

```

A(4,2) = -BETA(2,2)/BETA(2,1)

```

```

A(4,3) = -1.D0

```

```

C A(4,6) = -ALPHA(2,1)/BETA(2,1)

```

```

A(5,6) = 1.D0

```

```

A(6,1) = -ALPHA(1,2)/ALPHA(1,1)
A(6,4) = -BETA(1,1)/ALPHA(1,1)
N = 6
LDA = 6
LDE = 6
CALL DEVCCG(N,A,LDA,EVAL,EVEC,LDE)
DO 35 JJ = 1,6
SUM = 0.D0
DO 40 II = 1,6
40 SUM = SUM + CDABS(EVEC(II,JJ))*CDABS(EVEC(II,JJ))
SUM = DSQRT(SUM)
DO 45 II = 1,6
45 EVEC(II,JJ) = EVEC(II,JJ)/SUM
35 CONTINUE
C*****
RETURN
END
C*****
SUBROUTINE AMAT(EVAL,EVEC,PI,CMAT)
C*****
IMPLICIT REAL *8 (A-H,O-Z)
COMPLEX *16 CMAT(6,6),EVEC(6,6),EVAL(6),FACT(6)
DO 10 I = 1,6
10 FACT(I) = CDEXP(EVAL(I)*PI)
DO 20 I = 1,3
DO 20 J = 1,6
CMAT(I,J) = EVEC(I,J)
20 CMAT(I+3,J) = EVEC(I,J)*FACT(J)

```

```

RETURN
END
C*****
SUBROUTINE CINV(CMAT,DET)
C*****
IMPLICIT REAL *8 (A-H,O-Z)
COMPLEX*16 CMAT(6,6),FAC(6,6),DET1,DET
INTEGER IPVT(6)
N=6
LDA=6
LDF=6
C*****
C GET LU FACTORIAZATION TO SEND TO DETERMINANT ROUTINE
C*****
CALL DLFTCG(N,CMAT,LDA,FAC,LDF,IPVT)
C*****
CALL DLFDCG(N,FAC,LDF,IPVT,DET1,DET2)
C*****
C WRITE(6,100) DET1,DET2
C 100 FORMAT(2X,'DET1 = ',F15.7,5X,F15.7,/, ' DET2 = ',F15.7)
C*****
DET=DET1*10.D0**DET2
RETURN
END

```

Table 3. Sample Input

Temperature (C)	omega (Hz)
-70.000	4.7650003
-60.000	4.7279996
-50.000	4.6479997
-40.000	4.6420002
-30.000	4.6059999
-20.000	4.5769996
-10.000	4.5520000
0.000	4.5299997
10.000	4.5120000
20.000	4.4949998
30.000	4.4720001
40.000	4.4490003
50.000	4.4189996
60.000	4.3850002
70.000	4.3409996
80.000	4.2910003
90.000	4.2360000
100.000	4.1859998
110.000	4.1199998
120.000	3.9849996
130.000	3.6890001
140.000	3.4280004
150.000	3.2899999
160.000	3.2329998
170.000	3.2069997
180.000	3.1929998
190.000	3.1789999

Table 4. Sample Output

Temperature (C)	E sub z (GPa)
-70.00	16.239
-60.00	16.022
-50.00	15.515
-40.00	15.515
-30.00	15.225
-20.00	15.079
-10.00	14.935
0.00	14.789
10.00	14.645
20.00	14.572
30.00	14.427
40.00	14.282
50.00	14.064
60.00	13.847
70.00	13.630
80.00	13.340
90.00	12.977
100.00	12.687
110.00	12.324
120.00	11.527
130.00	9.932
140.00	8.627
150.00	7.902
160.00	7.685
170.00	7.539
180.00	7.467
190.00	7.395

**The two page vita has been
removed from the scanned
document. Page 1 of 2**

**The two page vita has been
removed from the scanned
document. Page 2 of 2**